

Review Article

Dark Matter: A Primer

Katherine Garrett and Gintaras Dūda

Department of Physics, Creighton University, 2500 California Plaza, Omaha, NE 68178, USA

Correspondence should be addressed to Gintaras Dūda, gkduda@creighton.edu

Received 12 June 2010; Accepted 28 September 2010

Academic Editor: David Merritt

Copyright © 2011 K. Garrett and G. Dūda. This is an open access article distributed under the Creative Commons Attribution License, which permits unrestricted use, distribution, and reproduction in any medium, provided the original work is properly cited.

Dark matter is one of the greatest unsolved mysteries in cosmology at the present time. About 80% of the Universe's gravitating matter is nonluminous, and its nature and distribution are for the most part unknown. In this paper, we will outline the history, astrophysical evidence, candidates, and detection methods of dark matter, with the goal to give the reader an accessible but rigorous introduction to the puzzle of dark matter. This paper targets advanced students and researchers new to the field of dark matter, and includes an extensive list of references for further study.

1. Introduction

One of the most astounding revelations of the twentieth century in terms of our understanding of the Universe is that ordinary baryonic matter, that is, matter made up of protons and neutrons, is not the dominant form of material in the Universe. Rather, some strange new form of matter, dubbed “dark matter,” fills our Universe, and it is roughly five times more abundant than ordinary matter. Although we have yet to detect this strange material in the laboratory, there is a great deal of evidence which points to the necessity of its existence.

A complete understanding of dark matter requires utilizing several branches of physics and astronomy. The creation of dark matter during the hot expansion of the Universe is understood through statistical mechanics and thermodynamics. Particle physics is necessary to propose candidates for dark matter and explore its possible interactions with ordinary matter. General relativity, astrophysics, and cosmology dictate how dark matter acts on large-scales and how the Universe may be viewed as a laboratory to study dark matter. Many other areas of physics come into play as well, making the study of dark matter a diverse and interdisciplinary field. Furthermore, the profusion of ground and satellite-based measurements in recent years have rapidly advanced the field making it dynamic and timely; we are truly entering the era of “precision cosmology”.

This paper aims to give a general overview of the subject of dark matter suitable for nonexperts; we hope to treat this fascinating and important topic in a way such that the non-specialist will gain a strong foundation and introduction to dark matter. It is at times difficult to find understandable and appropriate literature for individuals with no background on the subject. Existing reviews are either popular-level pieces which are too general or specialized pieces for experts in the field, motivating us to create an accessible overview. We particularly hope that this paper will be helpful to graduate students beginning their study of dark matter and to other physicists and astronomers who would like to learn more about this important topic.

To give such an introduction to dark matter, we will first briefly explain the first hints that dark matter exists, elaborate on the strong evidence physicists and astronomers have accumulated in the past years, discuss the neutralino and other possible candidates, and describe various detection methods used to probe the dark matter's mysterious properties. Although we will at times focus on supersymmetric theories of dark matter, other possibilities will be introduced and discussed.

2. History and Early Indications

Astronomers have long relied on photometry to yield estimates on mass, specifically through well-defined mass to

luminosity ratios (M/L). This is not at all surprising, since visual astronomy relies on the light emitted from distant objects. For example, the M/L ratio for the Sun is $M/L = 5.1 \times 10^3 \text{ kg/W}$; since this number is not terribly instructive, one usually measures mass to luminosity in terms of the Sun's mass and luminosity such that $M_\odot/L_\odot = 1$ by definition. Thus by measuring the light output of an object (e.g., a galaxy or cluster of galaxies) one can use well-defined M/L ratios in order to estimate the mass of the object.

In the early 1930s, Oort found that the motion of stars in the Milky Way hinted at the presence of far more galactic mass than anyone had previously predicted. By studying the Doppler shifts of stars moving near the galactic plane, Oort was able to calculate their velocities, and thus made the startling discovery that the stars should be moving quickly enough to escape the gravitational pull of the luminous mass in the galaxy. Oort postulated that there must be more mass present within the Milky Way to hold these stars in their observed orbits. However, Oort noted that another possible explanation was that 85% of the light from the galactic center was obscured by dust and intervening matter or that the velocity measurements for the stars in question were simply in error [1].

Around the same time Oort made his discovery, Swiss astronomer Zwicky found similar indications of missing mass, but on a much larger scale. Zwicky studied the Coma cluster, about 99 Mpc (322 million lightyears) from Earth, and, using observed Doppler shifts in galactic spectra, was able to calculate the velocity dispersion of the galaxies in the Coma cluster. Knowing the velocity dispersions of the individual galaxies (i.e., kinetic energy), Zwicky employed the virial theorem to calculate the cluster's mass. Assuming only gravitational interactions and Newtonian gravity ($F \propto 1/r^2$), the virial theorem gives the following relation between kinetic and potential energy:

$$\langle T \rangle = -\frac{1}{2} \langle U \rangle, \quad (1)$$

where $\langle T \rangle$ is the average kinetic energy and $\langle U \rangle$ is the average potential energy. Zwicky found that the total mass of the cluster was $M_{\text{cluster}} \approx 4.5 \times 10^{13} M_\odot$. Since he observed roughly 1000 nebulae in the cluster, Zwicky calculated that the average mass of each nebula was $M_{\text{nebula}} = 4.5 \times 10^{10} M_\odot$. This result was startling because a measurement of the mass of the cluster using standard M/L ratios for nebulae gave a total mass for the cluster approximately 2% of this value. In essence, galaxies only accounted for only a small fraction of the total mass; the vast majority of the mass of the Coma cluster was for some reason "missing" or nonluminous (although not known to Zwicky at the time, roughly 10% of the cluster mass is contained in the intracluster gas which slightly alleviates but does not solve the issue of missing mass) [2, 3].

Roughly 40 years following the discoveries of Oort, Zwicky, and others, Vera Rubin and collaborators conducted an extensive study of the rotation curves of 60 isolated galaxies [4]. The galaxies chosen were oriented in such a way so that material on one side of the galactic nucleus was approaching our galaxy while material on the other side

was receding; thus the analysis of spectral lines (Doppler shift) gave the rotational velocity of regions of the target galaxy. Additionally, the position along the spectral line gave angular information about the distance of the point from the center of the galaxy. Ideally one would target individual stars to determine their rotational velocities; however, individual stars in distant galaxies are simply too faint, so Rubin used clouds of gas rich in hydrogen and helium that surround hot stars as tracers of the rotational profile.

It was assumed that the orbits of stars within a galaxy would closely mimic the rotations of the planets within our solar system. Within the solar system,

$$v(r) = \sqrt{G \frac{m(r)}{r}}, \quad (2)$$

where $v(r)$ is the rotation speed of the object at a radius r , G is the gravitational constant, and $m(r)$ is the total mass contained within r (for the solar system essentially the Sun's mass), which is derived from simply setting the gravitational force equal to the centripetal force (planetary orbits being roughly circular). Therefore, $v(r) \propto 1/\sqrt{r}$, meaning that the velocity of a rotating body should decrease as its distance from the center increases, which is generally referred to as "Keplerian" behavior.

Rubin's results showed an extreme deviation from predictions due to Newtonian gravity and the luminous matter distribution. The collected data showed that the rotation curves for stars are "flat," that is, the velocities of stars continue to *increase* with distance from the galactic center until they reach a limit (shown in Figure 1). An intuitive way to understand this result is through a simplified model: consider the galaxy as a uniform sphere of mass and apply Gauss's law for gravity (in direct analogy with Gauss's Law for the electric field)

$$\int_S \vec{g} \cdot d\vec{A} = 4\pi G M_{\text{encl}}, \quad (3)$$

where the left hand side is the flux of the gravitational field through a closed surface and the right hand side is proportional to the total mass enclosed by that surface. If, as the radius of the Gaussian surface increases, more and more mass is enclosed, then the gravitational field will grow; here velocities can grow or remain constant as a function of radius r (with the exact behavior depending on the mass profile $M(r)$). If, however, the mass enclosed decreases or remains constant as the Gaussian surface grows, then the gravitational field will fall, leading to smaller and smaller rotational velocities as r increases. Near the center of the galaxy where the luminous mass is concentrated falls under the former condition, whereas in the outskirts of the galaxy where little to no additional mass is being added (the majority of the galaxy's mass being in the central bulge) one expects the situation to be that of the latter. Therefore, if the rotational velocities remain constant with increasing radius, the mass interior to this radius must be increasing. Since the density of luminous mass falls past the central bulge of the galaxy, the "missing" mass must be nonluminous. Rubin summarized, "The conclusion is inescapable: mass, unlike luminosity,

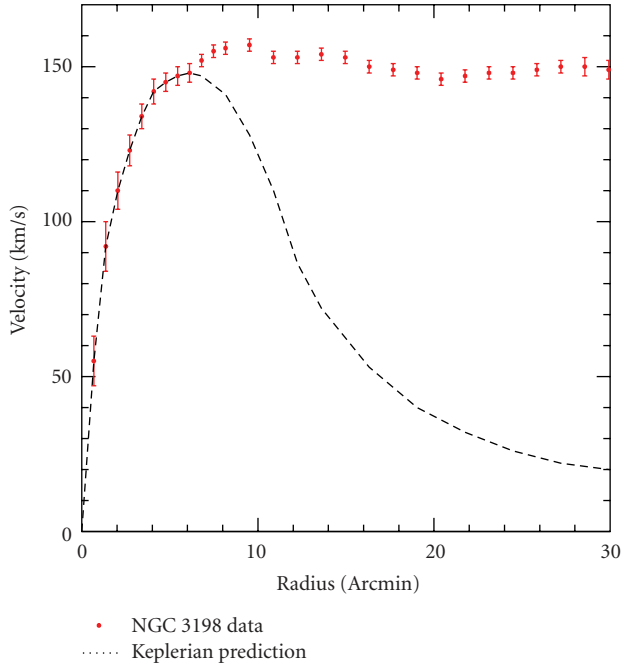


FIGURE 1: Measured rotational velocities of HI regions in NGC 3198 [5] compared to an idealized Keplerian behavior.

is not concentrated near the center of spiral galaxies. Thus the light distribution in a galaxy is not at all a guide to mass distribution” [4].

In the 1970s, another way to probe the amount and distribution of dark matter was discovered: gravitational lensing. Gravitational lensing is a result of Einstein’s Theory of Relativity which postulates that the Universe exists within a flexible fabric of spacetime. Objects with mass bend this fabric, affecting the motions of bodies around them (objects follow geodesics on this curved surface). The motions of planets around the Sun can be explained in this way, much like how water molecules circle an empty drain. The path of light is similarly affected; light bends when encountering massive objects. To see the effects of gravitational lensing, cosmologists look for a relatively close, massive object (often a cluster of galaxies) behind which a distant, bright object (often a galaxy) is located (there is actual an optimal lens-observer separation, so this must be taken into account as well). If the distant galaxy were to be located *directly* behind the cluster, a complete “Einstein ring” would appear; this looks much like a bullseye, where the center is the closer object and the ring is the lensed image of the more distant object. However, the likelihood of two appropriately bright and distant objects lining up perfectly with the Earth is low; thus, distorted galaxies generally appear as “arclets,” or partial Einstein rings.

In 1979, Walsh et al. were the first to observe this form of gravitational lensing. Working at the Kitt Peak National Observatory, they found two distant objects separated by only 5.6 arc seconds with very similar redshifts, magnitudes, and spectra [6]. They concluded that perhaps they were seeing the same object twice, due to the lensing of a closer,

massive object. Similar observations were made by Lynds and V. Petrosian in 1988, in which they saw multiple arclets within clusters [7].

We can study a distant galaxy’s distorted image and make conclusions about the amount of mass within a lensing cluster using this expression for θ_E , the “Einstein radius” (the radius of an arclet in radians)

$$\theta_E = \sqrt{\frac{4GM}{c^2} \frac{d_{LS}}{d_L d_S}}, \quad (4)$$

where G is the gravitational constant, M is the mass of the lens, c is the speed of light, and d_{LS} , d_L , and d_S are the distance between the lens and source, the distance to the lens, and the distance to the source, respectively (note: these distances are angular-diameter distances which differ from our “ordinarily” notion of distance, called the proper distance, due to the expansion and curvature of the Universe). Physicists have found that this calculated mass is much larger than the mass that can be inferred from a cluster’s luminosity. For example, for the lensing cluster Abell 370, Bergmann, Petrosian, and Lynds determined that the M/L ratio of the cluster must be about 10^2 – 10^3 solar units, necessitating the existence of large amounts of dark matter in the cluster as well as placing constraints on its distribution within the cluster [8].

3. Modern Understanding and Evidence

3.1. Microlensing. To explain dark matter physicists first turned to astrophysical objects made of ordinary, baryonic matter (the type of matter that we see every day and is made up of fundamental particles called quarks, which we will discuss in further detail in Section 4). Since we know that dark matter must be “dark,” possible candidates included brown dwarfs, neutron stars, black holes, and unassociated planets; all of these candidates can be classified as MACHOs (MASSIVE Compact Halo Objects).

To hunt for these objects two collaborations, the MACHO Collaboration and the EROS-2 Survey, searched for gravitational microlensing (the changing brightness of a distant object due to the interference of a nearby object) caused by possible MACHOs in the Milky Way halo. (Other collaborations have studied this as well, such as MOA, OGLE, and SuperMACHO [9–11]). The MACHO Collaboration painstakingly observed and statistically analyzed the skies for such lensing; 11.9 million stars were studied, with only 13–17 possible lensing events detected [12]. In April of 2007, the EROS-2 Survey reported even fewer events, observing a sample of 7 million bright stars with only *one* lensing candidate found [13]. This low number of possible MACHOs can only account for a very small percentage of the nonluminous mass in our galaxy, revealing that most dark matter cannot be strongly concentrated or exist in the form of baryonic astrophysical objects. Although microlensing surveys rule out baryonic objects like brown dwarfs, black holes, and neutron stars in our galactic halo, can other forms of baryonic matter make up the bulk of dark matter? The answer, surprisingly, is no, and the evidence behind this

claim comes from Big Bang Nucleosynthesis (BBN) and the Cosmic Microwave Background (CMB).

3.2. Cosmological Evidence. BBN is a period from a few seconds to a few minutes after the Big Bang in the early, hot universe when neutrons and protons fused together to form deuterium, helium, and trace amounts of lithium and other light elements. In fact, BBN is the largest source of deuterium in the Universe as any deuterium found or produced in stars is almost immediately destroyed (by fusing it into ${}^4\text{He}$); thus the present abundance of deuterium in the Universe can be considered a “lower limit” on the amount of deuterium created by the Big Bang. Therefore, by considering the deuterium to hydrogen ratio of distant, primordial-like areas with low levels of elements heavier than lithium (an indication that these areas have not changed significantly since the Big Bang), physicists are able to estimate the D/H abundance directly after BBN (it is useful to look at the ratio of a particular element’s abundance relative to hydrogen). Using nuclear physics and known reaction rates, BBN elemental abundances can be theoretically calculated; one of the triumphs of the Big Bang model is the precise agreement between theory and observational determinations of these light elemental abundances. Figure 2 shows theoretical elemental abundances as calculated with the BBN code `nuc123` compared with experimental ranges [14]. It turns out that the D/H ratio is heavily dependent on the overall density of baryons in the Universe, so measuring the D/H abundance gives the overall baryon abundance. This is usually represented by $\Omega_b h^2$, where Ω_b is the baryon density relative to a reference critical density (ρ_c) and $h = H/100 \text{ km sec}^{-1} \text{ Mpc}^{-1}$ (the reduced Hubble constant, which is used because of the large historical uncertainty in the expansion rate of the Universe). Cyburt calculated two possible values for $\Omega_b h^2$ depending on what deuterium observation is taken: $\Omega_b h^2 = 0.0229 \pm 0.0013$ and $\Omega_b h^2 = 0.0216^{+0.0020}_{-0.0021}$, both which we will see accounts for only about 20% of the total matter density [15].

The CMB, discovered by Penzias and Wilson in 1964 (but theorized by others much earlier) as an excess background temperature of about 2.73 K, is another way in which we can learn about the composition of the Universe [16]. Immediately after the Big Bang, the Universe was an extremely dense plasma of charged particles and photons. This plasma went through an initial rapid expansion, then expanded at a slower, decreasing rate, and cooled for about 380,000 years until it reached what is known as the epoch of recombination. At this time, neutral atoms were formed, and the Universe became transparent to electromagnetic radiation; in other words, photons, once locked to charged particles because of interactions, were now able to travel unimpeded through the Universe. The photons released from this “last scattering” exist today as the CMB.

COBE (COsmic Background Explorer) launched in 1989, verified two fundamental properties of the CMB: (1) the CMB is remarkably uniform (2.73 K across the sky) and (2) the CMB, and thus the early universe, is a nearly perfect blackbody (vindicating the use of statistical

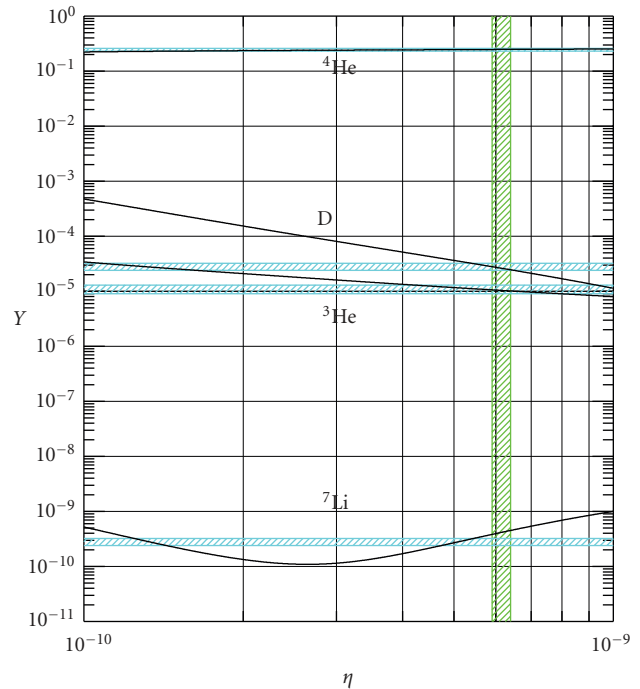


FIGURE 2: Light elemental abundances versus the photon to baryon ratio, η . The horizontal lines show measured abundances of the respective elements and the vertical lines show the photon to baryon ratio as measured by WMAP.

thermodynamics to describe the early universe). Although the CMB is extraordinarily uniform, COBE’s Differential Microwave Radiometer (DMR) discovered in its first year fundamental anisotropies (fluctuations) within the CMB, beyond the signal due to our motion relative to the CMB frame and foregrounds, such as emission from dust in the Milky Way. These fundamental fluctuations are due to two different effects. Large scale fluctuations can be attributed to the Sachs-Wolfe effect: lower energy photons are observed today from areas that were more dense at the time of last scattering (these photons, once emitted, lost energy escaping from deeper gravitational potential wells). On small scales, the origin of the CMB anisotropies are due to what are called acoustic oscillations. Before photon decoupling, protons and photons can be modeled as a photon-baryon fluid (since electrons are so much less massive than baryons we can effectively ignore them here). This fluid effectively goes through the following cycle: (1) the fluid is compressed as it falls into a gravitational well, (2) the pressure of the fluid increases until it forces the fluid to expand outward, (3) the pressure of the fluid decreases as it expands until gravity pulls it back, and (4) the process repeats until photon decoupling. Depending on the location in the cycle for a portion of the fluid at photon decoupling, the photons which emerge vary in temperature. The fluctuations in the CMB are thus indications of both the initial density perturbations that allowed for the formation of early gravitational wells as well as dynamics of the photon-baryon fluid. In this manner the temperature fluctuations of the CMB are dependent

on the amount of baryons in the Universe at the time of recombination.

Although the detection of the fluctuations in the CMB was a major accomplishment, the magnitude of the temperature variations puzzled scientists. These fundamental fluctuations in the CMB are incredibly small, only about $30 \pm 5 \mu\text{K}$, meaning that the CMB is uniform to 1 part in 10^5 . In fact, these fluctuations were too small to have solely accounted for the seeds of structure formation [17]; essentially, given the size of the CMB fluctuations, the structure of the Universe we see today would not have had time to form. The problem is time: ordinary matter only becomes charge neutral at the epoch of recombination, and before that, due to electrostatic forces, matter cannot effectively clump into gravitational wells to begin forming structure. The COBE results showed a need for an electrically neutral form of matter that could jump start the structure formation process well before recombination.

WMAP (Wilkinson Microwave Anisotropy Probe) was launched in 2001 with the mission to more precisely measure the anisotropies in the CMB. Located at the Earth-Sun L2 point (about a million miles from Earth), the satellite has taken data continuously (most recently having released an analysis of seven years of operation) and is able to detect temperature variations as small as one millionth of a degree. Due to the increased angular resolution of WMAP (and through the use of computer codes which can calculate the CMB anisotropies given fundamental parameters such as the baryon density), we now know the total and baryonic matter densities from WMAP [18]:

$$\Omega_m h^2 = 0.1334^{+0.0056}_{-0.0055}, \quad \Omega_b h^2 = 0.02260 \pm 0.00053, \quad (5)$$

where $\Omega_m h^2$ is the total matter density, and $\Omega_b h^2$ is the baryonic matter density. The first essential observation is that these two numbers are different; baryonic matter is not the only form of matter in the Universe. In fact, the dark matter density, $\Omega_{\text{dm}} h^2 = 0.1123 \pm 0.0035$, is around 83% of the total mass density. Locally, this corresponds to an average density of dark matter $\rho_{\text{dm}} \approx 0.3 \text{ GeV}/\text{cm}^3 \approx 5 \times 10^{-28} \text{ kg}/\text{m}^3$ at the Sun's location (which enhanced by a factor of roughly 10^5 compared to the overall dark matter density in the Universe due to structure formation). An analysis of the CMB allows for a discrimination between dark matter and ordinary matter precisely because the two components act differently; the dark matter accounts for roughly 85% of the mass, but unlike the baryons, it is not linked to the photons as part of the "photon-baryon fluid." Figure 3 demonstrates this point extremely well; small shifts in the baryon density result in a CMB anisotropy power spectrum (a graphical method of depicting the CMB anisotropies) which are wholly inconsistent with WMAP and other CMB experiment data.

Analyses of the large-scale structure of the Universe also yield evidence for dark matter and help break degeneracies present in the CMB data analysis. By calculating the distance to galaxies using their redshifts, cosmologists have been able to map out the approximate locations of more than 1.5 million galaxies. For example, the Sloan Digital Sky Survey

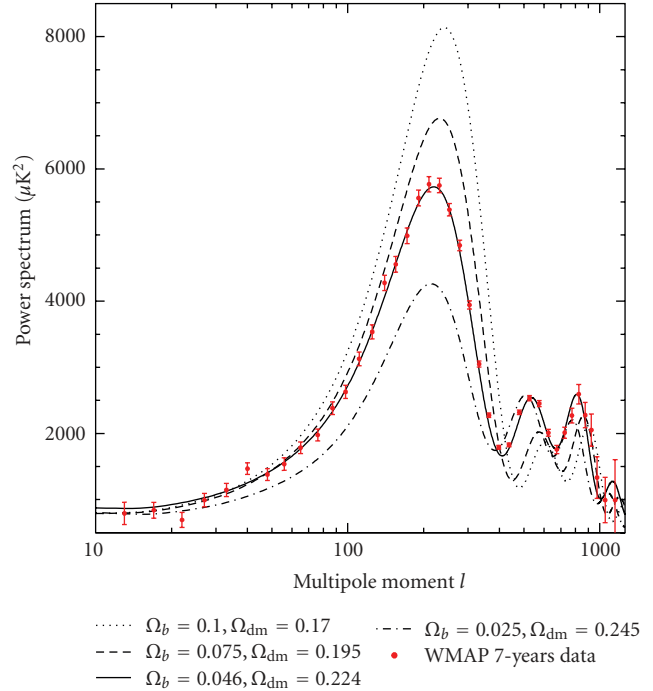


FIGURE 3: The CMB Anisotropy Power Spectrum for various values of Ω_b and Ω_{dm} (holding $\Omega_{\text{tot}} = 1$) with WMAP year 7 data. The anisotropy power spectrum gives the level of temperature fluctuations on patches of various angular scales, where a spherical version of a Fourier transform gives multipoles l , where roughly $l = 180^\circ/\theta$, with θ the angular scale in degrees.

(SDSS) has created 3D maps of more than 900,000 galaxies, 120,000 quasars, and 400,000 stars during its eight years of operation [19]. In fact, galaxy counts have had a long and important history in cosmology; in the 1950s and 60s radio galaxy counts provided the earliest, hard evidence against the Steady State model. But how can galaxy counts give evidence for dark matter? As discussed earlier, the current structure in the Universe is due to initial density fluctuations which served as seeds for structure formation magnified by the presence of dark matter. The most likely source of these initial density perturbations are quantum fluctuations magnified by inflation, a period of early rapid exponential growth approximately 10^{-35} seconds after the Big Bang. Under the assumption that these random fluctuations are Gaussian, a single function, the power spectrum $P(k)$, is sufficient to describe the density perturbations. From here a given $P(k)$ can be used to theoretically calculate large-scale structure. These statements are true, of course, only statistically. Furthermore, the converse is also true: by measuring large-scale structure (galaxy counts and surveys) one can experimentally determine the power spectrum $P(k)$. By obtaining the matter power spectrum from galaxy surveys, the amount of total matter and baryonic matter can be found: the peak of $P(k)$ is sensitive to the value of Ω_m , and the amount of baryons has effects on the shape of $P(k)$ (through baryonic acoustic oscillations, that is, excesses in galaxies

separated at certain distances due to sound waves in the pre-recombination plasma) [20]. Using these techniques, a final study of the 2dF Galaxy Redshift Survey power spectrum found $\Omega_m = 0.231 \pm 0.021$ and $\Omega_b/\Omega_m = 0.185 \pm 0.046$; a study based on data from SDSS yielded $\Omega_m = 0.286 \pm 0.018$ and $\Omega_{\text{dm}}h^2 = 0.02267 \pm 0.00058$ [21, 22]. Note that these results agree with both CMB and BBN predictions.

N -body simulations of large-scale structure are another tool which have been used to demonstrate the need for dark matter. These simulations often take weeks to complete on superclusters; for example, MS-II tracked over 10 billion particles which each represent $6.89 \times 10^6 h^{-1} M_\odot$ in a volume of $(100 h^{-1} \text{Mpc})^3$ to study dark matter halo structure and formation [23]. Similarly, Di Matteo et al. ran simulations to study the role of black holes in structure formation using 20–200 million particles in a volume of $(33.75 h^{-1} \text{Mpc})^3$ to $(50 h^{-1} \text{Mpc})^3$ [24]. N -body simulations confirm the need for dark matter. Simulations without dark matter do not form the familiar filament and void-type structures seen in the observable universe by SDSS and other surveys on the proper timescales. Additionally, scenarios run in which dark matter is relativistic or “hot” find that structure formation is retarded or “washed-out” instead of enhanced; thus not only is dark matter needed, but more specifically, dark matter must be “cold” or nonrelativistic during the period of structure formation [25, 26].

3.3. Most Recent Evidence. Recent evidence hailed as the “smoking-gun” for dark matter comes from the Bullet cluster, the result of a subcluster (the “bullet”) colliding with the larger galaxy cluster 1E 0657-56. During the collision, the galaxies within the two clusters passed by each other without interacting (a typical distance between galaxies is approximately one megaparsec, or 3.26 million lightyears). However, the majority of a cluster’s baryonic mass exists in the extremely hot gas between galaxies, and the cluster collision (at roughly six million miles per hour) compressed and shock heated this gas; as a result, a huge amount of X-ray radiation was emitted which has been observed by NASA’s Chandra X-ray Observatory. Comparing the location of this radiation (an indication of the location of the majority of the baryonic mass in the clusters) to a mapping of weak gravitational lensing (an indication of the location of the majority of the total mass of the clusters) shows an interesting discrepancy; the areas of strong X-ray emission and the largest concentrations of mass seen through gravitational lensing are not the same. The majority of the mass in the clusters is nonbaryonic and gravity “points” back to this missing mass [27].

The galaxy cluster known as MACS J0025.4-1222 is a second example of a powerful collision between two clusters which separated the luminous and dark matter within the two clusters. In mid-2008, Bradač et al. found that the behavior of the matter within this cluster is strikingly similar to the Bullet Cluster; the dark matter passed through the collision while the intergalactic gas interacted and emitted X-rays. These results reaffirmed those of the Bullet Cluster and the need for collisionless dark matter (as well as severely

constraining MOND theories (see the appendix for a brief description of MOND theories) [28].

In May of 2007, NASA’s Hubble Space Telescope (HST) detected a ring-like structure of dark matter, caused by another collision of two massive galaxy clusters one to two billion years ago [29]. The dark matter in the two clusters collapsed towards the center, but some of it began to “slosh” back out, causing the ring-shaped structure it now has. Overlapping the distribution of gravitational lensing with the baryonic mass in the combined cluster (just as with the Bullet cluster) shows the largest discrepancy yet between luminous and dark matter.

In early 2009, Penny et al. released results of a study from a HST survey of the Perseus Cluster, which is located about 250 million light years from Earth. They noticed that small, dwarf spheroidal galaxies are stable while larger galaxies are being torn apart by tidal forces caused by the cluster potential, a sign that a significant amount of dark matter may be holding the dwarf galaxies together. By determining the minimum mass required for these dwarf galaxies to survive the cluster potential, Penny et al. were able to calculate the amount of dark matter needed in each galaxy. They specifically studied 25 dwarf spheroidal galaxies within the cluster and found that 12 require dark matter in order to survive the tidal forces at the cluster center.

In conclusion, the evidence for dark matter on scales from dwarf galaxies to clusters to the largest scales in the Universe is compelling. There is remarkable agreement between multiple lines of evidence about the need for cold dark matter. Having established the need for dark matter, in the next section we will discuss possible particle candidates for dark matter and how theories beyond the Standard Model are necessary to solve the puzzle.

4. Particle Candidates

Although the existence of dark matter is well motivated by several lines of evidence, the exact nature of dark matter remains elusive. Dark matter candidates are generically referred to as WIMPs (Weakly Interacting Massive Particles); in other words, they are massive particles that are electrically neutral which do not interact very strongly with other matter. In this section we will explore some possible particle candidates for dark matter and the theories that lie behind them. But to begin with, we give a brief review of the Standard Model of particle physics.

4.1. The Standard Model and the Neutrino. The Standard Model (SM) is the quantum field theory that describes three of the four fundamental forces in nature: electricity and magnetism, the weak nuclear force, and the strong nuclear force. Gravitational interactions are not part of the SM; at energies below the Planck scale gravity is unimportant at the atomic level. There are sixteen confirmed particles in the SM, seven of which were predicted by the model before they were found experimentally, and one particle yet to be seen: the Higgs boson, which is believed to be the mediator of

the Higgs field responsible for giving all other SM particles mass. In the SM, there are six quarks (up, down, top, bottom, charm, and strange), six leptons (electron, mu, tau, and their respective neutrinos), and five force carriers (photons, gluons, W^\pm , Z , and the Higgs boson). Quarks and leptons are classified as fermions with half integer spins and are split into three generations, where force carriers are classified as gauge bosons with integer spins. Each of these particles also has a corresponding antiparticle, denoted with a bar (e.g., the up antiquark's symbol is \bar{u}), with opposite charge. Table 1 arranges the SM fundamental particles and some of their basic qualities.

SM particle interactions obey typical conservation of momentum and energy laws as well as conservation laws for internal gauge symmetries like conservation of charge, lepton number, and so on. The model has been thoroughly probed up to energies of ≈ 1 TeV, and has led to spectacular results such as the precision measurement of the anomalous magnetic moment of the electron (analogous to measuring the distance between New York and Los Angeles to the width of a human hair).

The final undiscovered particle, the Higgs boson, is thought to be extremely massive; the latest bounds from the CDF and DØ collaborations at the Tevatron have restricted the mass of the Higgs to two regions: 114–160 GeV and 170–185 GeV [31]. Since the Higgs boson couples very weakly to ordinary matter it is difficult to create in particle accelerators. Hopefully, the powerful Linear Hadron Collider (LHC) in Geneva, Switzerland, will confirm the existence of the Higgs boson, the final particle of the SM.

Despite its success, the SM does not contain any particle that could act as the dark matter. The only stable, electrically neutral, and weakly interacting particles in the SM are the neutrinos. Can the neutrinos be the missing dark matter? Despite having the “undisputed virtue of being known to exist” (as put so well by Lars Bergstrom), there are two major reasons why neutrinos cannot account for all of the Universe’s dark matter. First, because neutrinos are relativistic, a neutrino-dominated universe would have inhibited structure formation and caused a “top-down” formation (larger structures forming first, eventually condensing and fragmenting to those we see today) [32]. However, galaxies have been observed to exist less than a billion years after the Big Bang and, together with structure formation simulations, a “bottom-up” formation (stars galaxies then large galaxies then clusters, etc.) seems to be the most likely [33]. Second, Spergel et al. ruled out neutrinos as the entire solution to missing mass using cosmological observations: WMAP combined with large-scale structure data constrains the neutrino mass to $m_\nu < 0.23$ eV, which in turn makes the cosmological density $\Omega_\nu h^2 < 0.0072$ [18]. While neutrinos do account for a small fraction of dark matter, they clearly cannot be the only source.

The lack of a dark matter candidate does not invalidate the SM, but rather suggests that it must be extended. Perhaps the SM is only a valid theory at low energies, and that there is new physics “beyond the Standard Model;” that is, new theories may supplement, rather than replace, the SM. Such new theories have already been proposed, the most

promising being supersymmetry, which also yields a viable dark matter candidate called the neutralino or LSP.

4.2. Problems of the Standard Model. Although very successful, the SM has two flaws which hint at the need for new solutions: the hierarchy problem and the fine-tuning problem. The hierarchy problem arises from the SM’s prediction of the Higgs vacuum expectation value (vev, i.e., the average value of the field in the vacuum), which is about 246 GeV. Theorists have predicted that at high enough energies (≈ 1 TeV) the electromagnetic and weak forces act as a single unified force called the electroweak force (this has also been experimentally verified). However at smaller energies, the single unified force breaks down into two separate forces: the electromagnetic force and the weak force. It turns out that after this breaking, the Higgs field’s lowest energy state is not zero, but the 246 GeV vacuum expectation value. It is precisely this nonzero value that gives other particles mass through their interactions with the Higgs field. The 246 GeV vev is at the weak scale (the typical energy of electroweak processes); however, the Planck scale (the energy at which quantum effects of gravity become strong) is around 10^{19} GeV. The basic question, then, is why is the Planck scale 10^{16} times larger than the weak scale? Is there simply a “desert” between 10^3 and 10^{19} GeV in which no new physics enters?

There is an additional difficulty with the Standard Model. Most calculations in a quantum field theory are done perturbatively. For example, the scattering cross section of two electrons at a given energy can be calculated up to a certain power of α , the fine structure constant, which is the coupling constant for electromagnetism. The calculation is represented pictorially with Feynman diagrams; the number of particle interaction vertices is related to the power of α . However, virtual particles and more complicated diagrams can also contribute to the process with higher powers of α , several examples of which can be seen in Figure 4.

As an example, the best anomalous magnetic moment of the electron calculation involves 891 diagrams [34]. Thus most quantities have so-called “quantum-loop” corrections (although some quantities, like the photon’s mass, are protected by symmetries). The fine-tuning problem arises when trying to calculate the mass of the Higgs particle; quantum loop corrections to the Higgs mass are quadratically divergent. If one uses 10^{16} GeV as the scale at which the electroweak and strong forces combine to become a single unified force (which has been theorized but not seen), one requires an almost perfect cancellation on the order of 1 part in 10^{14} for the Higgs mass to come out at the electroweak scale (≈ 150 GeV). This unnatural cancellation is a source of alarm for theorists and signifies that we lack an understanding of physics beyond the SM.

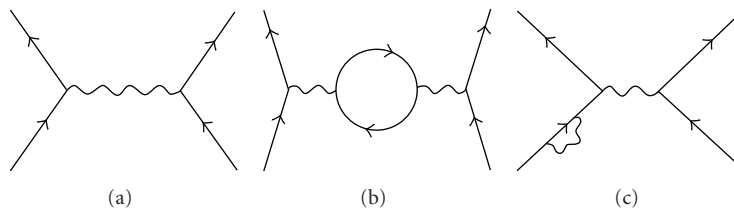
5. Supersymmetry

One possible extension to the Standard Model is supersymmetry (SUSY). SUSY at its essence is an additional symmetry between fermions and bosons and can best be

TABLE 1: The particles predicted by the Standard Model. Approximate masses of particles as last reported by the Particle Data Group [30].

(a) Fermions								
Generation 1			Generation 2			Generation 3		
Particle	Mass (MeV)	Charge	Particle	Mass (MeV)	Charge	Particle	Mass (MeV)	Charge
up quark (u)	2.55	$+\frac{2}{3}$	charm quark (c)	1270	$+\frac{2}{3}$	top quark (t)	171200	$+\frac{2}{3}$
down quark (d)	5.04	$-\frac{1}{3}$	strange quark (s)	104	$-\frac{1}{3}$	bottom quark (b)	4200	$-\frac{1}{3}$
electron (e^-)	0.511	-1	muon (μ^-)	105.7	-1	tau (τ^-)	1776.8	-1
e neutrino (ν_e)	$<2.0 \times 10^{-6}$	0	μ neutrino (ν_μ)	<0.19	0	τ neutrino (ν_τ)	<18.2	0

(b) Gauge Bosons					
Particle	Force	Acts through	Acts on	Mass (MeV)	Charge
Photon (γ)	Electromagnetic	Electric charge	Electrically charged particles	$<1 \times 10^{-24} \approx 0$	0
Z boson (Z)	Weak nuclear	Weak interaction	Quarks and leptons	91188	0
W^\pm bosons (W^\pm)	Weak nuclear	Weak interaction	Quarks and leptons	80398	± 1
Gluon (g)	Strong nuclear	Color charge	Quarks and gluons	0	0
Higgs boson (H^0)	Higgs force	Higgs field	Massive particles	>114400	0

FIGURE 4: The tree level diagram on the left represents the electron-electron scattering process to the lowest order in perturbation theory. The two graphs on the right represent higher order processes (which can be thought of as loop corrections) and enter with higher powers of α .

understood by beginning with the Coleman-Mandula theorem. The Coleman-Mandula theorem states that the most general symmetries that a quantum field theory (QFT) can possess are Lorentz invariance (special relativity) and gauge symmetries like conservation of charge, lepton number, and so on. (whose generators belong to Lie Algebras [35]). In other words, the Coleman-Mandula theorem is a “no-go” theorem: a relativistic QFT can have no other symmetries. In particular, there can be no change of the spin of particles. That is, there is no way in the SM to change fermions to bosons or vice-versa.

However, in the mid-1970s two groups of physicists realized that the Coleman-Mandula theorem can be evaded. Supersymmetry evades the restriction of the Coleman-Mandula theorem by generalizing and loosening the restriction on the types of symmetries of a QFT (in addition to Lie Algebras one can consider graded Lie Algebras whose operators anticommute). This additional symmetry allows for the interconversion of fermions and bosons. Essentially, every fermion is now associated with a superpartner boson and every boson with a superpartner fermion; adding supersymmetry to the standard model effectively doubles the number of particles. Although doubling the number of particles may seem a hopeless complication, supersymmetry is very attractive theoretically for a number of reasons.

To begin with, supersymmetry may solve the hierarchy and the fine-tuning/naturalness problem in the Standard Model. SUSY is new physics which acts at energies beyond the SM which helps to explain why the electroweak and Planck energy scales are so different. In terms of the fine-tuning problem, SUSY can explain why the Higgs mass and the Higgs vev are so small. If SUSY were an exact symmetry of nature, then the mass of each SM bosonic particle must be equal to its superpartner fermion mass. And since boson and fermion mass corrections in QFT calculations enter with opposite signs, they can cancel each other leading to a “naturally” small Higgs mass and vev. Of course supersymmetry is a broken symmetry, meaning that the symmetry is no longer valid at the typical energies and background temperatures in the Universe today. For example, we do not see a bosonic superpartner to the electron with .511 MeV mass which would be a sign of unbroken supersymmetry. Due to this breaking (which is not well understood) all superpartners must be extremely massive (much like the W and Z particles acquire mass in electroweak symmetry breaking while the photon remains massless). In order to produce acceptable corrections to the Higgs mass, the difference between boson and fermion masses must be of the order of 1 TeV.

Furthermore, precision measurements of Standard Model parameters at the LEP collider show that using only the Standard Model particle content the strong, weak, and electromagnetic forces do not seem to unify at energies of about 10^{16} GeV. Particle physicists have long predicted that like the weak and electromagnetic forces which unify at energies of about 10^3 GeV, the three quantum forces should merge to become a single Grand Unified Force. However, if one adds the minimal particle content of supersymmetry, the couplings indeed seem to converge at a unification scale of $M \simeq 2 \times 10^{16}$ GeV [36–38]. Additionally, supersymmetry is inherent in string theory, which currently is the only theory which has the possibility of unifying the quantum world with gravity.

And finally, and this is perhaps the most appealing characteristic of supersymmetry, the Standard Model with SUSY does in fact offer a viable dark matter candidate which we will discuss shortly. The new particles generated by adding SUSY to the SM are shown below in Table 2.

When examining the particle content of the SM with SUSY, there are several possible particles which could act as dark matter. These are the neutralino (a particle state which is a superposition of the neutral superpartners of the Higgs and gauge bosons), the sneutrino (the superpartner of the neutrino), and the gravitino (the superpartner of the graviton which would come from a quantum theory of gravity). All of these particles are electrically neutral and weakly interacting, and thus are ideal WIMP-like candidates for dark matter. However, sneutrinos annihilate very rapidly in the early universe, and sneutrino relic densities are too low to be cosmologically significant [39, 40]. And gravitinos act as hot dark matter rather than cold dark matter, and large-scale structure observations are inconsistent with a universe dominated by hot dark matter [41, 42]. This leaves the neutralino as a viable candidate.

But how can the neutralino, an extremely massive particle, exist today in sufficient numbers to make up the bulk of the dark matter (generically, massive particles decay into lighter ones)? The answer lies in what is called R-parity. In the Standard Model symmetries guarantee baryon and lepton number conservation; for this reason, the proton, the lightest baryon, cannot decay. However, with the addition of supersymmetry, this is no longer generally true due to the presence of squarks and sleptons; recall, SUSY changes quarks and leptons into bosons and vice-versa, so baryon and lepton number are violated as a matter of course. However, we know that the amount of baryon and lepton number violation (at least at low energies) must be extremely small due to sensitive tests. An interesting property of SUSY is that if one writes down a theory without lepton and baryon number violating terms, no such terms will ever appear, even through quantum loop corrections (another advantage of SUSY is that certain types of quantities never get loop corrections). Under this assumption, a new symmetry, called R-parity, may be conserved by a SUSY version of the SM. We assign +1 R-parity for all Standard Model fields (including both Higgs fields), and -1 R-parity for all superpartners. The immediate consequence of R-parity conservation is that because there are an even number of SUSY particles in every

interaction, the lightest supersymmetric partner, the LSP, is stable and will not decay. If this LSP is neutral, it is an excellent candidate for dark matter.

In most SUSY versions of the standard model, the neutralino is the LSP and seems to be the most promising dark matter candidate; the relic abundance of neutralinos can be sizeable and of cosmological significance, and detection rates are high enough to be accessible in the laboratory but not high enough to be experimentally ruled out. Thus the SM with SUSY offers a single dark matter candidate: the neutralino. Although at present not one supersymmetric particle has been detected in the laboratory, supersymmetry currently offers the best hope of modeling and understanding dark matter. One clear advantage is that the minimal extension of the Standard Model using supersymmetry is well understood, and calculations, including dark matter densities and detection rates, can be performed.

6. Exotic Candidates

Although the neutralino and SUSY are well-motivated, other particle candidates for dark matter also exist. The axion is a particle proposed in 1977 by Roberto Peccei and Helen Quinn to solve the so-called “strong-CP problem” [43]. In a nutshell, the strong force Lagrangian contains a term that can give an arbitrarily large electric dipole moment to the neutron; since no electric dipole moment for the neutron has ever been observed, Peccei and Quinn postulated that a new symmetry prevents the appearance of such a term (much like a gauge symmetry keeps the photon massless). They further theorized that this symmetry is slightly broken which leads to a new, very light scalar particle, the axion. Although this particle is extremely light (theories place its mass in the μeV range), it can exist in sufficient numbers to act as cold dark matter. Since axions should couple to photons, axions can be searched for with precisely tuned radio frequency (RF) cavities; inside the magnetic field of an RF cavity the axion can be converted into a photon which shows up as excess power in the cavity. And in a unique blend of particle and astrophysics, limits on axions have been placed through observations of red giant stars; axions, if they existed, would offer another cooling mechanism which can be constrained by studying how quickly red giant stars cool [44]. Although the axion has never been observed directly, several experiments such as ADMX and CARRACK are continuing the search and setting new limits on axion parameters [45, 46].

If axions exist and SUSY is also correct, then the axino (the supersymmetric partner of the axion) is by a wide margin the LSP; neutralinos would decay into axinos through $\chi \rightarrow \tilde{a} + \gamma$ [47]. However, axinos would also act as hot dark matter and thus could not compose the bulk of the dark matter.

One final exotic particle candidate for dark matter comes from theories of extra spatial dimensions. The idea that our universe could have extra spatial dimensions began in the 1920s with Theodor Kaluza and Oscar Klein; by writing down Einstein’s general theory of relativity in five

TABLE 2: The particles predicted by a supersymmetric extension of the Standard Model. Limits on the masses of particles as last reported by the Particle Data Group [30].

(a) Sfermions								
Generation 1			Generation 2			Generation 3		
Particle	Mass (GeV)	Charge	Particle	Mass (GeV)	Charge	Particle	Mass (GeV)	Charge
up squark (\tilde{u})	>379	$+\frac{2}{3}$	charm squark (\tilde{c})	>379	$+\frac{2}{3}$	top squark (\tilde{t})	>92.6	$+\frac{2}{3}$
down squark (\tilde{d})	>379	$-\frac{1}{3}$	strange squark (\tilde{s})	>379	$-\frac{1}{3}$	bottom squark (\tilde{b})	>89	$-\frac{1}{3}$
selectron (\tilde{e})	>73	-1	smuon ($\tilde{\mu}$)	>94	-1	stau ($\tilde{\tau}$)	>81.9	-1
e sneutrino ($\tilde{\nu}_e$)	>95	0	μ sneutrino ($\tilde{\nu}_\mu$)	>94	0	τ sneutrino ($\tilde{\nu}_\tau$)	>94	0

(b) Gauginos		
Particle	Mass (GeV)	Description
Neutralinos ($\tilde{\chi}_{1-4}^0$)	>46	Mixture of photino ($\tilde{\gamma}$), zino (\tilde{Z}), and neutral higgsino (\tilde{H}^0)
Charginos ($\tilde{\chi}_{1,2}^\pm$)	>94	Mixture of winos (\tilde{W}^\pm) and charged higgsinos (\tilde{H}^\pm)
Gluinos (\tilde{g})	>308	Superpartner of the gluon

dimensions, they were able to recover four dimensional gravity as well as Maxwell's equations for a vector field (and an extra scalar particle that they didn't know what to do with) [48, 49]. Klein explained the nonobservation of this extra fifth dimension by compactifying it on a circle with an extremely small radius (something like 10^{-35} cm so that it is completely nonobservable). Kaluza-Klein theories (as they came to be known) were an initial quest for a grand unified theory; however, the emergence of the weak and strong nuclear forces as fundamental forces of nature relegated this type of approach to unification to the drawing board. However, in the late 1990s two new scenarios with extra dimensions appeared. Arkani-Hamed, Dvali, and Dimopoulos tried to solve the hierarchy problem by assuming the existence of large extra dimensions (initially on the scale of mm or smaller); they made the bold assertion that the electroweak scale is the only fundamental scale in nature and that the Planck scale appears so small due to the presence of these extra dimensions [50]. Lisa Randall and Raman Sundrum, on the other hand, proposed infinitely large extra dimensions that were unobservable at low energies; gravity, they explained, was weak precisely because it was the only force that could "leak-out" into this extra dimension [51].

What do extra dimensions have to do with candidates for dark matter? In theories in which extra dimensions are compactified, particles which can propagate in these extra dimensions have their momenta quantized as $p^2 \sim 1/R^2$, where p is the particle's momentum and R is the size of the extra dimension (we also use natural units where $\hbar = c = 1$). Therefore, for each particle free to move in these extra dimensions, a set of fourier modes, called Kaluza-Klein states, appears

$$m^2 = \frac{n^2}{R^2} + m_0^2, \quad (6)$$

where R is the size of the compactified extra dimension, m_0 is the regular standard model mass of the particle, and

n is the mode number. Each standard model particle is then associated with an infinite tower of excited Kaluza-Klein states. If translational invariance along the fifth dimension is postulated, then a new discrete symmetry called Kaluza-Klein parity exists and the Lightest Kaluza-Klein particle (LKP) can actually be stable and act as dark matter; in most models the LKP is the first excitation of the photon. Working within the framework of the Universal Extra Dimensions (UED) model [52], Servant and Tait showed in 2003 that if the LKP has mass between 500 and 1200 GeV, then the LKP particle can exist in sufficient numbers to act as the dark matter [53]. Additional motivations for extra dimensional theories of dark matter include proton stability and the cancellation of gauge anomalies from three generations of fermions [54].

Many other theories have been proposed to account for the Universe's dark matter, most of which are not as promising as those already discussed. These include Q-balls, WIMPzillas, branons, and GIMPs [55–57]. However, the neutralino remains the most studied and most theoretically motivated dark matter candidate. In the next section we will discuss how particles like the neutralino (the SUSY LSP) can be produced in the early universe and how to determine if they exist today in sufficient density to act as the dark matter.

7. Production in the Early Universe

7.1. Review of Big Bang Cosmology. To understand how dark matter particles could have been created in the early universe, it is necessary to give a brief review of the standard model of cosmology. The standard model of cosmology, or the "Big Bang Theory" in more colloquial language, can be summed up in a single statement: the Universe has expanded adiabatically from an initial hot and dense state and is isotropic and homogeneous on the largest scales. Isotropic here means that the Universe looks the same in every

direction and homogeneous that the Universe is roughly the same at every point in space; the two points form the so-called cosmological principle which is the cornerstone of modern cosmology and states that “every comoving observer in the cosmic fluid has the same history” (our place in the Universe is in no way special). The mathematical basis of the model is Einstein’s general relativity and it is experimentally supported by three key observations: the expansion of the Universe as measured by Edwin Hubble in the 1920s, the cosmic microwave background, and Big Bang Nucleosynthesis.

The Friedmann equations are the result of applying general relativity to a four dimension universe which is homogeneous and isotropic:

$$\begin{aligned} H^2 + \frac{k}{a^2} &= \frac{8\pi G}{3}\rho, \\ \dot{\rho} &= -3H(p + \rho), \\ \frac{d}{dt}(sa^3) &= 0, \end{aligned} \quad (7)$$

where H is the Hubble constant (which gives the expansion rate of the Universe and is not really a constant but changes in time), k is the spatial curvature of the Universe today, G is Newton’s gravitation constant, and p and ρ are the pressure and energy density respectively of the matter and radiation present in the Universe. a is called the scale-factor which is a function of time and gives the relative size of the Universe (a is defined to be 1 at present and 0 at the instant of the Big Bang), and s is the entropy density of the Universe. The Friedmann equations are actually quite conceptually simple to understand. The first says that the expansion rate of the Universe depends on the matter and energy present in it. The second is an expression of conservation of energy and the third is an expression of conservation of entropy per comoving volume (a comoving volume is a volume where expansions effects are removed; a nonevolving system would stay at constant number or entropy density in comoving coordinates even through the number or entropy density is in fact decreasing due to the expansion of the Universe).

The expansion rate of the Universe as a function of time can be determined by specifying the matter or energy content through an equation of state (which relates energy density to pressure). Using the equation of state $\rho = wp$, where w is a constant one finds

$$a(t) \propto \left(\frac{t}{t_0}\right)^{2/3(1+w)}, \quad (8)$$

where t_0 represents the present time such that $a(t_0) = 1$ as stated earlier. For nonrelativistic matter where pressure is negligible, $w = 0$ and thus $a \propto t^{2/3}$; and for radiation (and highly relativistic matter) $w = 1/3$ and thus $a \propto t^{1/2}$. Although the real universe is a mixture of nonrelativistic matter and radiation, the scale factor follows the dominant contribution; up until roughly 47,000 years after the Big Bang, the Universe was dominated by radiation and hence the scale factor grows like $t^{1/2}$. Since heavy particles like dark matter were created before nucleosynthesis (which occurred

minutes after the Big Bang), we shall treat the Universe as radiation dominated when considering the production of dark matter.

7.2. Thermodynamics in the Early Universe. Particle reactions and production can be modeled in the early universe using the tools of thermodynamics and statistical mechanics. In the early universe one of the most important quantities to calculate is the reaction rate per particle

$$\Gamma = n\sigma v, \quad (9)$$

where n is the number density of particles, σ is the cross section (the likelihood of interaction between the particles in question), and v is the relative velocity. As long as $\Gamma \gg H(t)$ we can apply equilibrium thermodynamics (basically this measures if particles interact frequently enough or is the expansion of the Universe so fast that particles never encounter each other). This allows us to describe a system macroscopically with various state variables: V (volume), T (temperature), E (energy), U (internal energy), H (enthalpy), S (entropy), and so on. These variables are path independent; so long as two systems begin and end at the same value of a state variable, the change in that variable for both systems is the same. The most relevant quantity in the early universe is temperature. Since time and temperature are inversely correlated, that is, the early universe is hotter (the exact relationship is that $T \propto 1/a$), we can re-write the Hubble constant and reaction rates and cross sections in terms of temperature. The temperature will also tell us if enough thermal energy is available to create particles; for example, if the temperature of the Universe is 10 GeV, sufficient thermal energy exists to create 500 MeV particles from pair production, but not 50 GeV particles.

Statistical thermodynamics can be used to derive relations for the energy density, number density, and entropy density of particles in the early universe in equilibrium. To do so, Bose-Einstein statistics are used to describe distributions of bosons and Fermi-Dirac statistics are used to describe distributions of fermions. The main difference between the two arises from the Pauli exclusion principle which states that no two identical fermions can occupy the same quantum state at the same time. Bosons, on the other hand, *can* occupy the same quantum state at the same time. Hence there are small differences in the quantities we compute for bosons and fermions. To obtain the relevant statistical quantities, we begin with the distribution factor. The distribution factor $f_i(p)$, which gives the relative numbers of particles with various values of momentum p for a particle species i , is given by

$$f_i(p) = \frac{1}{e^{(E_i - \mu_i)/T} \pm 1}, \quad (10)$$

where $E_i = \sqrt{m_i^2 + p^2}$, μ_i is the chemical potential of species i (energy associated with change in particle number), and the +1 case describes bosons and the -1 case fermions. (You might notice that the Boltzmann constant k is missing from the denominator of the exponential. To simplify things,

cosmologists use a system of units where $\hbar = k = c = 1$.) The distribution factor can be used to determine ratios and fractions of particles at different energies, as well as the number and energy densities which are given by the integrals

$$\begin{aligned} n_i &= \frac{g_i}{(2\pi)^3} \int f_i(p) d^3p = \frac{g_i}{2\pi^2} \int p^2 f_i(p) dp, \\ \rho_i &= \frac{g_i}{(2\pi)^3} \int E_i f_i(p) d^3p = \frac{g_i}{2\pi^2} \int p^2 E_i f_i(p) dp, \end{aligned} \quad (11)$$

where $d^3p = 4\pi p^2 dp$ and g_i is the number of degrees of freedom. The degrees of freedom are also called the statistical weights and basically account for the number of possible combinations of states of a particle. For example, consider quarks. Quarks have two possible spin states and three possible color states, and there are two quarks per generation. So, the total degrees of freedom for the quarks in the Standard Model are $g_q = 2 \times 3 \times 2 = 12$ with an addition $g_{\bar{q}} = 12$ for the antiquarks. Each fundamental type of particle (and associated antiparticle) has its own number of degrees of freedom, which enter into the calculations of number and energy densities. The known particles of the SM (plus the predicted Higgs boson) have a total of 118 degrees of freedom.

The integrals for number and energy densities can be solved explicitly in two limits: (1) the relativistic limit where $m \ll T$ and (2) the nonrelativistic limit where $m \gg T$. For nonrelativistic particles where $m \gg T$,

$$n_{NR} = g_i \left(\frac{mT}{2\pi} \right)^{3/2} e^{-m/T}, \quad (12)$$

which is a Maxwell-Boltzmann distribution (no difference between fermions and bosons) and

$$\rho_{NR} = m n. \quad (13)$$

For relativistic particles, on the other hand, where $m \ll T$,

$$n_R = \begin{cases} \frac{\zeta(3)}{\pi^2} g_i T^3 & \text{for bosons,} \\ \frac{3}{4} \frac{\zeta(3)}{\pi^2} g_i T^3 & \text{for fermions,} \end{cases} \quad (14)$$

$$\rho_R = \begin{cases} \frac{\pi^2}{30} g_i T^4 & \text{for bosons,} \\ \frac{7}{8} \frac{\pi^2}{30} g_i T^4 & \text{for fermions,} \end{cases} \quad (15)$$

where ζ is the Riemann Zeta function. These results show that at any given time (or temperature) only relativistic particles contribute significantly to the total number and energy density; the number density of nonrelativistic species are exponentially suppressed. As an example, knowing that the CMB photons have a temperature today of 2.73 K, we can use (14) to calculate $n_\gamma \approx 410$ photons/cm³.

7.3. Particle Production and Relic Density: The Boltzmann Equation. In the early universe, very energetic and massive particles were created and existed in thermal equilibrium (through mechanisms like pair production or collisions/interactions of other particles). In other words, the

processes which converted heavy particles into lighter ones and vice versa occurred at the same rate. As the Universe expanded and cooled, however, two things occurred: (1) lighter particles no longer had sufficient kinetic energy (thermal energy) to produce heavier particles through interactions and (2) the Universe's expansion diluted the number of particles such that interactions did not occur as frequently or at all. At some point, the density of heavier particles or a particular particle species became too low to support frequent interactions and conditions for thermal equilibrium were violated; particles are said to "freeze-out" and their comoving number density (no longer affected by interactions) remains constant. The exact moment or temperature of freeze-out can be calculated by equating the reaction rate, (9), with the Hubble (expansion) rate. The density of a specific particle at the time of freeze-out is known as the relic density for this particle since its abundance remains constant (see Figure 5).

We know that a supersymmetric particle like the neutralino is a good dark matter candidate: it is electrically neutral, weakly interacting, and massive. It is also produced copiously in the early universe. But can a particle like the neutralino (or a generic WIMP) still exist in the present day universe with sufficient density to act as dark matter? To answer this question we will explore how precisely to compute relic densities.

The Boltzmann equation gives an expression for the changing number density of a certain particle over time, dn/dt . To formulate the Boltzmann equation for a particle species, relevant processes must be understood and included. For supersymmetric particles, like the neutralino, there are four: (1) the expansion of the Universe, (2) coannihilation, in which two SUSY particles annihilate with each other to create standard model particles, (3) decay of the particle in question, and (4) scattering off of the thermal background. Each of these processes then corresponds respectively to a term in the Boltzmann equation for dn_i/dt where there are N SUSY particles

$$\begin{aligned} \frac{dn_i}{dt} &= -3Hn_i - \sum_{j=1}^N \langle \sigma_{ij} v_{ij} \rangle (n_i n_j - n_i^{\text{eq}} n_j^{\text{eq}}) \\ &\quad - \sum_{j \neq i} \left[\Gamma_{ij} (n_i - n_i^{\text{eq}}) - \Gamma_{ji} (n_j - n_j^{\text{eq}}) \right] \\ &\quad - \sum_{j \neq i} \left[\langle \sigma'_{Xij} v_{ij} \rangle (n_i n_X - n_i^{\text{eq}} n_X^{\text{eq}}) \right. \\ &\quad \left. - \langle \sigma'_{Xji} v_{ji} \rangle (n_j n_X - n_j^{\text{eq}} n_X^{\text{eq}}) \right]. \end{aligned} \quad (16)$$

In the case of supersymmetry (which we will focus on for the rest of this section) the Boltzmann equation can be simplified by considering R-parity. If we also assume that the decay rate of SUSY particles is much faster than the age of the Universe, then all SUSY particles present at the beginning of the Universe have since decayed into neutralinos, the LSP. We can thus say that the abundance of neutralinos is the sum of the density of all SUSY particles ($n = n_i + \dots + n_N$). Note, then, that when we take the sum in (16), the third and fourth

terms cancel. This makes sense, because conversions and decays of SUSY particles do not affect the overall abundance of SUSY particles (and therefore neutralinos), and thus make no contribution to dn/dt . We are left with

$$\frac{dn}{dt} = -3Hn - \langle \sigma_{\text{eff}} v \rangle (n^2 - n_{\text{eq}}^2), \quad (17)$$

where n is the number density of neutralinos, $\langle \sigma_{\text{eff}} v \rangle$ is the thermal average of the effective annihilation cross section σ_{eff} times the relative velocity v , and n_{eq} is the equilibrium number density of neutralinos. A quick note should be made about the thermal average $\langle \sigma_{\text{eff}} v \rangle$ and the added difficulty behind it. As thoroughly described by Schelke, coannihilations between the neutralinos and heavier SUSY particles can cause a change in the neutralino relic density of more than 1000%, and thus should not be left out of the calculation [58]. The thermal average is then not just the cross section times relative velocity of neutralino-neutralino annihilation, but of neutralino-SUSY particle annihilations as well; many different possible reactions must be considered based upon the mass differences between the neutralino and other SUSY particles.

By putting (17) in terms of $Y = n/s$ and $x = m_\chi/T$ where T is the temperature to simplify the calculations, we obtain the form

$$\frac{dY}{dx} = -\sqrt{\frac{\pi}{45G}} \frac{g_*^{1/2} m_\chi}{x^2} \langle \sigma_{\text{eff}} v \rangle (Y^2 - Y_{\text{eq}}^2), \quad (18)$$

where $g_*^{1/2}$ is a parameter which depends on the effective degrees of freedom. Equation (18) can then be integrated from $x = 0$ to $x_0 = m_\chi/T_0$ to find Y_0 (which will be needed in (19) for the relic density) [59].

Figure 5 (adapted from Kolb and Turner's excellent treatment of this topic [60]) plots an analytical approximation to the Boltzmann Equation and illustrates several key points. The y -axis is essentially (or at least proportional to) the relic density; the solid line is the equilibrium value and the dashed-line is the actual abundance. Notice that at freeze-out, the actual abundance leaves the equilibrium value and remains essentially constant; the equilibrium value, on the other hand, continues to decrease so freeze-out is key to preserving high relic densities. Furthermore, the larger the annihilation cross section, $\langle \sigma_a v \rangle$, the lower the relic density; this makes sense since the more readily a particle annihilates, the less likely it will exist in large numbers today. This has been paraphrased by many as "the weakest wins" meaning that particles with the smallest annihilation cross sections will have the largest relic densities.

Using the value of Y_0 described above, the relic density of neutralinos is given by

$$\Omega_\chi h^2 = \frac{h^2 m_\chi s_0 Y_0}{\rho_{\text{crit}}} = 2.755 \times 10^8 \frac{m_\chi}{\text{GeV}} Y_0, \quad (19)$$

where m_χ is the mass of the neutralino, s_0 is the entropy density today (which is dominated by the CMB photons since there are about 10^{10} photons per baryon in the Universe),

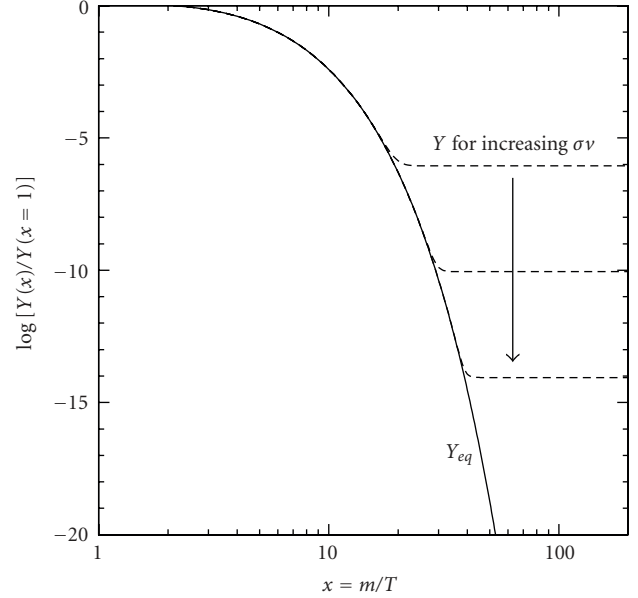


FIGURE 5: The evolution of $Y(x)/Y(x = 1)$ versus $x = m/T$ where $Y = n/s$.

and Y_0 is the result of integrating the modified version of the Boltzmann equation. For a more thorough discussion of the Boltzmann equation and the relic density of neutralinos, consult Schelke and Edsjö and Gondolo [58, 61].

Recall that the difference between the matter and baryon densities (as determined by WMAP) was $\Omega_\chi h^2 = 0.11425 \pm 0.00311$. Can particle models of dark matter like SUSY or Kaluza-Klein theories produce dark matter in sufficient quantities to act as the bulk of the dark matter? The answer generically is yes. Although SUSY theories cannot predict a single dark matter relic density due to the inherent uncertainty in the input parameters, the Standard Model plus supersymmetry does produce a wide range of models some of which have the expected dark matter density. For example, MSSM models (the minimal supersymmetric standard model) yield dark matter relic densities from 10^{-6} of the WMAP results to some which overclose the Universe; neutralino masses for the models which give a correct relic abundance typically lie in the range 50–1000 GeV. A similar calculation can be performed for Kaluza-Klein dark matter in the Universal Extra Dimension scenario; Hooper and Profumo report that with the first excitation of the photon as the LKP a relic abundance can be obtained in the proper range of $0.095 < \Omega_{\text{dm}} < 0.129$ for LKP masses between 850 and 900 GeV [52].

To summarize, statistical thermodynamics allows us to model conditions in the early universe to predict relic abundances of dark matter particles like neutralinos. What is remarkable is that such models produce dark matter abundances consistent with the range provided by cosmological measurements. Theories like SUSY and Kaluza-Klein theories are so powerful, in particular, because such calculations (even given a wide range of uncertainty in

several parameters) are possible. Armed with the required relic density of dark matter and the various models proposed by theorists, experiments can search for dark matter in specific areas of allowed parameter space. In the next section we will discuss the methods and progress of the various detection schemes and experiments.

8. Detection Schemes

Detecting (or creating) dark matter is key in determining its properties and the role of dark matter in the formation of structure in the Universe. Many experiments have searched and are currently searching for a signal of WIMP-like dark matter (many specifically for neutralinos) and each uses a different detection method. Although producing dark matter in a particle accelerator would be ideal (we would have better control and the experiment would be repeatable), but other methods to find dark matter, coined direct and indirect detection, also continue to be important in the search. Due to the summary nature of this paper, only a brief overview of this large topic will be presented here. For a more thorough review of detection techniques and results, refer to Baudis and Klapdor-Kleingrothaus for direct detection and Carr et al. for indirect [62, 63]. In this discussion we have assumed that the local dark matter distribution is at rest in the Milky Way halo. However, other possibilities, including dark matter clumps and velocity streams due to incomplete virialization are possible [64].

8.1. Production in Accelerators. Producing and detecting dark matter particles in an accelerator would be a huge step toward confirming the existence of dark matter (though it would not, intriguingly, verify that the produced particle acts as the vast amount of dark matter in the Universe detected through astrophysical means; in principle, dark matter in the Universe need not be comprised of a single component). If we assume that R-parity is conserved and that the dark matter is the neutralino and thus the LSP, then a signal in an accelerator will have several distinctive features. When SUSY particles are created, they will decay to the LSP and most likely escape the detector (similar to a neutrino—remember SUSY particles interact very weakly with regular matter). As the LSP leaves the collision space, it will carry with it energy and momentum which can be detected as missing energy and momentum. Similar signatures of missing energy would be detected if the dark matter were Kaluza-Klein excitations or other exotic particles.

Although direct evidence for SUSY or other exotic particles hasn't been seen yet, there are certain processes which depend heavily on whether they exist. For example, the radiative quark decay process ($s \rightarrow b\gamma$) and the anomalous magnetic moment of the muon constrain the possible masses of SUSY particles. The constraints obtained from these and other experiments, however, are highly model dependent so it is therefore difficult to make any general claims about them. Since there is such uncertainty in the theory, we will generically refer in the following sections to dark matter particles as WIMPs (Weakly Interacting Massive Particles).

8.2. Direct Detection. The basic idea of direct detection is simple: set up a very sensitive device, containing a large amount of some element, which can detect very small motions and interactions of the atoms within it. If dark matter is everywhere in the Universe, then it should be traveling around (and through) the Earth, and therefore a detection apparatus, at all times. Although dark matter is weakly interacting, it may occasionally bump into the nucleus of a detector atom and deposit some energy which can be sensed by the detector. To get an idea of how much energy a WIMP would deposit, we first estimate that WIMPs are moving at velocities of about 220 km/s and their masses are somewhere around 100 GeV. We then crudely find a WIMP's kinetic energy using

$$T = \frac{1}{2}mv^2 = \frac{1}{2}(1.783 \times 10^{-25} \text{ kg})(220,000 \text{ m/s})^2 \quad (20)$$

$$\approx 4.314 \times 10^{-15} \text{ J} \approx 26.9 \text{ keV}.$$

This is the upper limit of energy that a 100 GeV neutralino traveling at 220 km/s could deposit in the detector; the actual amount would almost certainly be smaller, since it is unlikely for a weakly-interacting particle to be completely stopped within the detector. Natural radioactivity generally emits MeV energies, making a keV increase in energy due to nuclear scattering nearly impossible to find. For this reason, direct detection devices must be radioactively clean and shielded from particles that may make detection of WIMPs difficult.

The recoil energy E of a WIMP with mass m scattering off of a nucleus of mass M can be more precisely found with the expression

$$E = \frac{\mu^2 v^2}{M}(1 - \cos \theta), \quad (21)$$

where $\mu = mM/(m + M)$ is the reduced mass, v is the speed of the WIMP relative to the nucleus, and θ is the scattering angle.

A WIMP signal should have specific characteristics. First, events should be uniformly distributed throughout the detector given that the local dark matter density is thought to be fairly homogeneous and the cross section of interaction remains constant. Secondly, a WIMP-nucleus interaction should be a single-site event, whereas an event from cosmic rays or naturally occurring radioactivity can be multisite. For this reason, detectors have an "anticoincidence veto system" which makes sure events that occur extremely close together (within nanoseconds), suggesting that they are caused by the same incoming particle, are not counted as caused by other WIMPs. Detection rates should also vary at different times of the year due to the Earth moving with or against the velocity of dark matter in the galaxy. This depends on the Earth's velocity, given by

$$v_E = 220 \text{ km/s} (1.05 + 0.07 \cos(\omega(t - t_0))), \quad (22)$$

where ω is $2\pi/\text{year}$ and t_0 is June 2. As a result, the variation of WIMP flux over a year is only about 7%, meaning that many events would be required to see such a small

modulation. These among other indications help detection experiments decide whether received signals really are WIMPs or not.

The interaction of a WIMP with the detector material can be classified by two characteristics: elastic or inelastic, and spin-dependent or spin-independent.

- (i) Elastic and inelastic scattering: Elastic scattering is the interaction of a WIMP with the nucleus as a whole. This causes the nucleus to recoil and, as we have seen, would deposit energies of around 25 keV. In inelastic scattering all of the energy does not go into nuclear recoil; instead the nucleus is excited to a higher energy state (e.g., the $5/2^+$ state in ^{73}Ge) which then decays by photon emission. If the excited state is long-lived enough, the decay signal can be separated from the nuclear recoil event; this leads to better background discrimination. However, inelastic scattering cross sections are generally smaller than elastic scattering cross sections due to a lack of coherence (the interaction is with individual nucleons rather than with the nucleus as a whole) [65].
- (ii) Spin-dependent and spin-independent scattering: Spin-dependent (“axial-vector”) scattering results from the coupling of a WIMP’s spin with the spin content of a nucleon. Spin-independent (“scalar”) does not depend on this and has the advantage of higher cross sections with larger nuclei (because of coherence where the WIMP interacts with the nucleus as a whole).

A recoil event can then be further categorized, taking on one of three forms.

- (i) Phonon/Thermal: a vibration (detected as a rise in temperature) in the crystal lattice of the detector, caused by the slight movement of a nucleus off which a WIMP has recoiled. An extremely sensitive thermometer system is located around the detector, allowing any temperature variation to be recorded.
- (ii) Ionization: an incident particle gives an electron in the detector enough energy to escape the pull of its nucleus. A small electric field is set up in the detector to “push” the new charge to a detector wall where it can be registered and counted as an ionization event.
- (iii) Scintillation: caused when an electron absorbs enough energy to climb to a higher energy state. After a short time, the electron will lose this energy by emitting a photon, which is then gathered by photomultipliers and converted to an electric signal so it can be analyzed.

A detector is generally set up to sense two of these WIMP signals. By doing so, background events can be recognized on an event-by-event basis and discarded, allowing possible dark matter signatures to be counted and analyzed.

To calculate the number of recoil events N expected in a detector within a range of recoil energy (E_1, E_2) , we take a sum over the nuclear species i in the detector

$$N_{E_1-E_2} = \sum_i \int_{E_1}^{E_2} \frac{dR_i}{dE} \epsilon_i(E) dE, \quad (23)$$

where dR_i/dE is the expected recoil rate per unit mass of i per unit nucleus recoil energy and per unit time, and $\epsilon_i(E)$ is the effective exposure of i in the detector. dR_i/dE is given by

$$\frac{dR_i}{dE} = \frac{\rho \sigma_i |F_i(E)|^2}{2m\mu_i^2} \int_{v > \sqrt{M_i E/2\mu_i^2}} \frac{f(\vec{v}, t)}{v} d^3v, \quad (24)$$

where ρ is the local halo dark matter density, σ_i is the WIMP-nucleus cross section, $F_i(E)$ is the nuclear form factor which takes into account that a nucleus is not a simple point particle, m is the WIMP mass, μ_i is the reduced mass, v is the velocity of the WIMP with respect to the detector, M_i is the mass of a nucleus of species i , E is the recoil energy, and $f(\vec{v}, t)$ is the WIMP velocity distribution (generally assumed to be a Maxwell-Boltzmann distribution) in the reference frame of the detector. The nuclear physics uncertainties are locked into $F_i(E)$ while the astrophysical uncertainties lie in the WIMP velocity distribution. $\epsilon_i(E)$ is given by

$$\epsilon_i(E) = \mathcal{M}_i T_i \epsilon_i(E), \quad (25)$$

where \mathcal{M} is the total mass of nuclei of species i in the detector that has been active for a time T_i , and $\epsilon_i(E)$ is the counting efficiency for nuclear recoils of energy E .

We can see from these expressions that a detector should ideally have a large mass with which to receive signals, be operational for a long period of time, and be properly shielded against background radiation. An upper limit can be put on the WIMP-nucleus cross section by comparing expected events (using the above expressions) to observation. Any negative results from direct detection experiments are not wasted time and effort; instead, we can say that the WIMP does not exist in a certain tested area of the parameter space (for a given dark matter theory) and look toward more sensitive areas. Fortunately, experiments are reaching more advanced detection techniques and are approaching the parameter space in which WIMPs are believed to exist.

While many others are in operation worldwide, the three direct detection experiments which have yielded the best (most constrained) results for the spin-independent WIMP-nucleus cross section are the Cryogenic Dark Matter Search (CDMS II) in the Soudan Mine, the UK Dark Matter Collaboration’s ZEPLIN-I (ZonEd Proportional scintillation in LIquid Noble gases) in the Boulby Mine, and XENON10 at the Gran Sasso Underground Laboratory.

Each of these three collaborations uses a different method to look for WIMPs. CDMS II uses a set of 250 gram Ge detectors and 100 gram Si detectors cooled to less than 50 mK. Each apparatus is classified as a ZIP (Z-dependent Ionization and Phonon) detector. While WIMPs recoil off of nuclei, background particles scatter off of electrons; the ZIP detectors are able to discriminate between the two events [66]. ZEPLIN-III uses the scintillation properties of liquid Xe

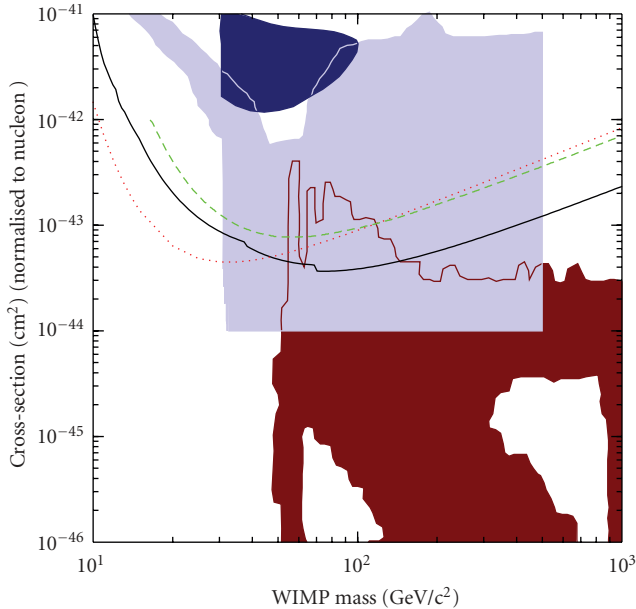


FIGURE 6: Spin-independent cross section versus WIMP mass with exclusion curves. The blue (top shaded) area is the DAMA claimed discovery region. The remaining shaded areas are regions of parameter space in which theory predicts dark matter candidates. The exclusion curves are: dashed—ZEPLIN III, solid line—CDMS II, dotted line—XENON 10. Models above the exclusion curves are experimentally ruled out. This plot was produced with the Dark Matter Limit Plot Generator [69].

to detect WIMPs, shielded by lead and a liquid scintillator veto to reduce background radiation [67]. XENON10 also uses liquid Xe to detect scintillation and ionization events [68]. The exclusion curves from these collaborations are shown in Figure 6. In Figure 6, the nature and extent of the shaded regions from theory depend heavily on the individual supersymmetric theories; we mean only to show here that there are theories which predict WIMP candidates that are within the reach of current and planned direct detection experiments.

One experiment, the DAMA collaboration, detected an annual modulation in scattering events that is around the expected 7% [70]. This is puzzling, however, because no other direct detection experiment has found such a signal. Gondolo and Gelmini have given possible reasons for this; for example, the WIMP velocity may be larger than the DAMA thresholds, but smaller than the thresholds of other detectors [71]. However, DAMA’s conclusions still remain controversial.

Other collaborations focusing on spin-independent direct detection include CRESST and EDELWEISS [72, 73]. Many other future projects have been proposed, such as GENIUS and SuperCDMS, which is planned to be able to probe nearly all split-supersymmetry model parameter space [74, 75].

Although spin-independent scattering has larger interaction rates in most SUSY models, spin-dependent scattering can explore the parameter space where scalar interaction

is less probable. For this reason, experiments searching for spin-dependent interactions have been able to set competitive upper limits on WIMP interactions. For example, ^{73}Ge makes up 7.73% of the CDMS Collaboration’s natural germanium detectors, and ^{29}Si accounts for 4.68% of the natural silicon, both which have nonzero spin. As a result, CMDS’s spin-dependent experiments have placed the best current upper limit on WIMP-neutron interactions [76]. Other direct detection experiments employing spin-dependent techniques include PICASSO and NAIAD [77, 78].

8.3. Indirect Detection. In supersymmetry, for example, neutralinos are classified as Majorana particles (they are their own antiparticle) and therefore annihilate with each other, giving off various products which we can detect. Hence a potential signal for the existence of dark matter is WIMP-WIMP annihilation. This technique is called “indirect detection” since we are not actually detecting the WIMPs themselves. Because the annihilation rate of WIMPs is proportional to the square of the dark matter density ($\Gamma_A \propto \rho_{\text{DM}}^2$), natural places to look for dark matter annihilations are those expected to have high WIMP densities, such as the Sun, Earth, and galactic center. Annihilation products include gamma-rays, neutrinos, and antimatter.

8.3.1. Gamma-Rays. Gamma-rays from WIMP annihilation are believed to occur most frequently in the galactic center. One way this process can take place is through a WIMP annihilation yielding a quark and antiquark, which then produce a particle jet from which a spectrum of gamma-rays is released. The quark antiquark fragmentation process has been thoroughly studied at accelerators and is well understood; the creation and propagation of gamma rays from such a jet is a fairly predictable process (compared to, for example, the “random walk” of charged antimatter particles through space). A second form of gamma-ray production is the decay of WIMPs directly to gamma-rays, ($\chi\chi \rightarrow \gamma\gamma$ or γZ), which produces gamma-rays (a “gamma-ray line”) that are proportional to the mass of the WIMPs involved. Since typical WIMP masses can be on the order of 100s of GeV, these are extremely high energy gamma rays. Although the flux is small and quite difficult to detect, observing such a gamma-ray line would be an obvious indication for dark matter annihilation and the WIMP mass (often referred to as the “smoking gun”).

As a gamma-ray enters an indirect detection device, it first passes through an anticoincidence shield which limits the amount of charged particles entering the detector. The gamma-ray then encounters “conversion foils,” which are thin sheets of heavy nuclei that convert the photon to a e^+e^- pair. A calorimeter tracks the energies of the positron and electron, while particle tracking detectors measure their trajectories. The signature of a gamma-ray event is then a registered energy with nothing triggering the anticoincidence shield, and the indication of two particles (the positron and electron) coming from the same location.

The EGRET Collaboration reported an excess of gamma-rays in 1998, pointing toward already accepted characteristics of dark matter: a 50–70 GeV WIMP mass and a ring of concentrated dark matter at a radius of 14 kpc from the galactic center (which would nicely answer for our flat rotation curves) [79]. This discovery is initially encouraging, but as Bergström et al. have shown, observed antiproton fluxes would have to be much larger if these excess gamma rays are being produced by neutralino or generic WIMP self annihilation [80]. For this reason and others, EGRET's results remain controversial.

8.3.2. Neutrinos. Neutrinos can be another important product of WIMP annihilation. As WIMPs travel through the Universe and through matter, they lose small amounts of energy due to scattering off of nuclei. Therefore, WIMPs can gather at the centers of large gravitating bodies, increasing their density until their annihilation rate equals half the capture rate (two WIMPs are needed for annihilation, where only one is needed for capture). For many of the primary particle physics models, the WIMP annihilation and capture rates are at (or nearly at) equilibrium in the Sun, a conveniently “close” object to observe. This equilibrium should allow for a steady annihilation rate, and therefore a constant flow of neutrinos emanating from within the Sun (we study only the neutrinos and not other products of annihilation because neutrinos interact so weakly that most escape from the Sun or body in question). Why not, then, study neutrinos coming from WIMP annihilations within the Earth, an even closer gravitating body? The earth (in most models) has not reached such an equilibrium and thus does not provide a flux of neutrinos; it is less massive than the Sun, so it causes less WIMP scattering and a much smaller gravitational potential well. Neutrino telescopes therefore usually focus on neutrino flux coming from the Sun, rather than the Earth.

The differential neutrino flux from WIMP annihilation is given by

$$\frac{dN_\nu}{dE_\nu} = \frac{\Gamma_A}{4\pi D^2} \sum_f B_X^f \frac{dN_\nu^f}{dE_\nu} \quad (26)$$

where Γ_A is the annihilation rate of WIMPs in the Sun and/or Earth, D is the distance of the detector from the source (the central region of the Sun and/or Earth), f is the WIMP pair annihilation final states, and B_X^f are the branching ratios of the final states. dN_ν^f/dE_ν are the energy distributions of neutrinos generated by the final state f [81]. Depending on the WIMP's mass and composition, annihilation processes include $\chi\chi \rightarrow t\bar{t}, b\bar{b}, c\bar{c}, ZZ, W^+W^-,$ and $\tau^+\tau^-$, which then decay to neutrinos among other products. For neutralinos or generic WIMPs lighter than W^\pm , annihilation to $b\bar{b}$ and $\tau^+\tau^-$ are the most common processes, yielding neutrinos with energies around 30 GeV. WIMPs with higher masses annihilate to Higgs and gauge bosons, top and bottom quarks, and muons, leading to neutrinos of masses that are much easier to detect (about half of the WIMP mass). Detection, then, depends heavily on the WIMP mass, as well

as the annihilation rate, density within the Sun, and other factors.

As neutrinos pass through the Earth, they sometimes interact with the hydrogen and oxygen and other atoms around the optical modules of a neutrino detector. Electrons, muons, and taus produced by such events are extremely energetic and are traveling faster than the speed of light in the medium; the particles are then detected optically due to the Cherenkov radiation they emit.

Because neutrinos are so weakly interacting, neutrino telescopes must be massive to detect a significant signal. AMANDA-II is a neutrino detector 1500 to 2000 meters underground within the ice of the South Pole where Cherenkov radiation can travel and be seen easily by optical modules. This experiment has not detected statistically significant results from the direction of the Sun, but has placed helped place firm limits on the muon flux [82]. A future experiment (expected to be fully completed in 2011), IceCube, will integrate AMANDA into a much larger detection experiment, with 7200 optical modules and a detector volume of a cubic kilometer [83]. Super-Kamiokande (“Super-K”) is another indirect detection experiment, located underground in the Kamioka-Mozumi mine in Japan. The detector consists of 50,000 tons of water and detects Cherenkov radiation from incoming muons as well. Super-K looks in the direction of the Sun, earth, and galactic center, and, like AMANDA, has not detected any excess of muon rates above the expected background [84].

8.3.3. Antimatter. Antimatter can be an excellent signal of WIMP annihilation precisely because antimatter is relatively rare cosmically, and many of the astrophysical processes which create antimatter are well understood. For example, the annihilation of WIMPs can also produce antiprotons via $\chi\chi \rightarrow q\bar{q}$ through hadronization (where the dominate annihilation process yields b quarks and antiquarks), and positrons through secondary products of the annihilation such as W^+W^- (and ZZ), where W (or Z) $\rightarrow e^+ \nu_e$. Unlike gamma-rays and neutrinos, these products are charged and thus affected by magnetic fields within space and also lose energy due to inverse Compton and synchrotron processes, so we cannot make any conclusions about where the annihilations occurred. We therefore study the flux of antimatter particles from the galactic halo as a whole, rather than assumed dense areas such as the galactic center or large bodies.

Experiments searching for antimatter must be located near the top of the Earth's atmosphere; various other cosmic rays and their consequential particle showers create too large and uncertain of a background to make conclusive analyses. It is important, however, to still consider and subtract any background caused by cosmic rays that reach the edges of our atmosphere. In 1994, the HEAT Collaboration detected an excess of cosmic ray positrons of energies around 10 GeV possibly caused by neutralino self-annihilation, and confirmed this signal again in 2000 [85, 86]. A “boost factor,” however, must be applied to the WIMP annihilation rate of a smooth halo in order to match the HEAT data; this

is perhaps an indication that we exist within an extremely clumpy halo, or that there are other unknown sources of antimatter. The Balloon-borne Experiment with Superconducting Spectrometer (BESS) also detected antiprotons with energies up to 4 GeV during its nine flights over several years [87].

Quite recently, the results from the PAMELA (a Payload for Antimatter Matter Exploration and Light-nuclei Astrophysics) satellite-borne experiment's flight from July 2006–February 2008 were released. The collaboration found that the positron fraction increases sharply over much of the range of 1.5–100 GeV and thus concluded that a primary source, either an astrophysical object or dark matter annihilation, must be present to account for the abundance of cosmic-ray positrons [88]. The data from PAMELA also require heavy WIMP candidates or large boost factors associated with nonuniform clumps in the dark matter distribution, thus constraining the nature of the possible dark matter. ATIC (Advanced Thin Ionization Calorimeter), a balloon-based experiment, also reported an excess of e^- or e^+ at 300–800 GeV. However, recent results from Fermi [89] and HESS [90] (the High Energy Stereoscopic System, a set of four Cherenkov telescopes in Namibia) do not see the same electron-positron excess of ATIC leaving the issue far from settled (however, Fermi does see an excess similar to that seen by PAMELA). Further data is necessary to determine if excess gamma ray and antimatter fluxes are indeed signals of dark matter annihilation or signatures of local astrophysical objects and backgrounds.

9. Conclusion and Challenges

The astrophysical and cosmological evidence for dark matter is both impressive and compelling. What is perhaps the most striking are the multiple lines of evidence which point to the need for dark matter. Elemental abundances from Big Bang Nucleosynthesis and fundamental anisotropies in the Cosmic Microwave Background Radiation both predict very similar baryon (ordinary matter) abundances, yet each describes a completely separate era in the history of the Universe in which very different physical processes are occurring. Dark matter is necessary to both describe galaxies and clusters of galaxies, and is a necessary ingredient in the formation of large-scale structure. It is this concordance of evidence that makes dark matter more than just a “fudge-factor”; although strange and unexpected, dark matter seems to be a fundamental and necessary component of our universe.

Although the composition and nature of dark matter is still unknown, theories like Supersymmetry or Kaluza-Klein theories of extra dimensions provide solid frameworks for attempting to understand dark matter. Of all of the particle candidates for dark matter, perhaps the best motivated is the neutralino. It is a typical WIMP: electrically neutral, weakly interacting, and massive, and through statistical mechanics in the early universe we can calculate abundances for the neutralino today which are consistent with it acting as the dark matter. Other exotic candidates for dark matter exist from axions to Q-balls to WIMPzillas. However outlandish

the candidate, the hunt for dark matter continues. The Large Hadron Collider at CERN will begin collisions at 3.5 TeV per beam in 2009–2010, ramping up to 7 TeV per beam most likely in 2011 and beyond, and will search for indications of supersymmetry and dark matter. Indirect searches continue to hunt for gamma rays and antimatter which might provide evidence for dark matter; the current controversy between PAMELA and ATIC and FERMI and HESS results demonstrate the advances and challenges in indirect detection. And finally, direct detection experiments continue to set more stringent limits on neutralino and WIMP scattering cross sections; these limits, as new technology is applied, are set to improve dramatically in the next decade with experiments like Super CDMS, GENIUS, and ZEPLIN IV.

Dark matter, of course, is not completely understood and faces challenges. The primary challenge is that it remains undetected in the laboratory. Another tension for dark matter is that it seems to possess too much power on small scales (~ 1 –1000 kpc). Numerical simulations of the formation of dark matter halos were performed by Klypin et al. and show that, to explain the average velocity dispersions for the Milky Way and Andromeda, there should be five times more dark matter satellites (dwarf galaxies with a very small ordinary matter content) with circular velocity >10 –20 km/s and mass $>3 \times 10^8 M_\odot$ within a 570 kpc radius than have been detected [91]. In other words, although dark matter is crucial in forming structure, current models form *too much* structure. Another study, from Moore et al., shows that dark matter models produce more steeply rising rotation curves than we see in many low surface brightness galaxies, again suggesting that simulations produce an overabundance of dark matter [92]. Of course, discrepancies on small scales may be entirely due to astrophysical processes; for example, photo-heating during reionization and/or supernova feedback particularly affect dwarf galaxies [93, 94]. Although important to consider, these challenges faced by dark matter are dwarfed by the compelling evidence for the necessity of dark matter along with its successes in explaining our universe. What makes this field so rich and vibrant is that work and research continue, and these challenges will lead to deeper understanding in the future.

Dark matter is an opportunity to learn more about the fundamental order of the Universe. Dark matter provides a tantalizing glimpse beyond the highly successful Standard Model of particle physics. The discovery of neutralinos would prove the validity of supersymmetry and help bridge the “desert” between the electroweak and the Planck scales. But ultimately, we look at dark matter as a mystery, one which will hopefully inspire physics and astronomy students in and out of the classroom. As Einstein said, “The most beautiful thing we can experience is the mysterious. It is the source of all true art and all science.”

Appendix

MOND Theories as Alternatives to Dark Matter

One alternative to dark matter, particularly as an explanation for the nonKeplerian motions of rotating bodies, is called

MOND (MODified Newtonian Dynamics). In 1983 Milgrom proposed that the flat rotation curves observed in many galaxies may be explained without postulating any sort of missing mass in the Universe [95]. He instead introduced an acceleration constant to modify Newton's second law, which would at small accelerations account for the radius independent nature of stellar motion.

Rather than the usual $\vec{F} = m\vec{a}$, the equation at the heart of MOND is

$$\vec{F} = m\mu\left(\frac{a}{a_0}\right)\vec{a}, \quad (\text{A.1})$$

$$\mu(x \gg 1) \approx 1, \quad \mu(x \ll 1) \approx x,$$

where \vec{F} is the force acting on an object of mass m and acceleration $a = |\vec{a}|$, and $a_0 \approx 2 \times 10^{-8} \text{ cm s}^{-2}$ is the acceleration constant determined by Milgrom (many other MOND theories have emerged with differing values for a_0). For accelerations greater than or equal to a_0 (most accelerations we see in every day life, including the motions of planets within our solar system), $x \approx 1$, and Newtonian dynamics can be used as usual. However, for very small accelerations such as for the orbits of objects far away from the galactic center, a_0 becomes significant; this is how MOND predicts and explains the flat rotation curves.

To demonstrate how MOND can explain flat rotation curves, we first consider the expression for the force of gravity \vec{F} on a star and Milgrom's modification of Newton's second law

$$\vec{F} = \frac{GMm}{r^2} = m\mu\left(\frac{a}{a_0}\right)\vec{a}, \quad (\text{A.2})$$

where G is the gravitational constant, m and M are the masses of the star and galaxy respectively, and r is the radius of the star's orbit. If we cancel m from both sides and assume that $\mu(a/a_0) = (a/a_0)$ at a very large r , we are left with

$$\frac{GM}{r^2} = \frac{a^2}{a_0}. \quad (\text{A.3})$$

Solving for a and using the relationship of acceleration with velocity and radius ($a = v^2/r$), we find

$$a = \frac{\sqrt{GMa_0}}{r} = \frac{v^2}{r}, \quad \text{and therefore,} \quad (\text{A.4})$$

$$v = \sqrt[4]{GMa_0},$$

where v has no dependence on r . This relation has allowed various studies to use MOND to fit flat rotation curves quite successfully for several low and high surface brightness galaxies (LSB and HSB galaxies, resp.) based on luminous mass alone [96–98]. As MOND predicts, LSB galaxies show a larger departure from Newtonian dynamics where HSB galaxies show discrepancies only in their outer regions where gravitational attraction is considerably smaller. MOND and TeVeS (the MONDian version of General Relativity) [99] have had success in predicting and describing other observed

galactic dynamics as well. For a recent review, see Sanders [100].

Despite these successes, MOND faces several major and critical challenges it has not been able to overcome. For example, when considering galaxy clusters, MOND cannot account for density and temperature profiles and requires unseen matter [101]. Evidence for dark matter exists on many distance scales and MOND essentially only works on galactic scales. Also, extremely low acceleration experiments (below a_0) have been conducted, finding no departure from Newton's second law and thus constraining MOND to reduce to Newton's second law in laboratory conditions [102, 103]. And finally, gravitational lensing evidence such as in the Bullet Cluster show that, in effect, the gravitational force points back not towards regular, observed baryonic matter but rather some form of dark matter which is not observed optically. MOND theories in their current forms cannot account for such a discrepancy easily, although more recent theories which wed MOND with a sterile neutrino are being developed [104]. However, for the above reasons and others, we feel that dark matter is a more promising solution to the puzzle of missing mass in the Universe.

Acknowledgment

K. Garrett and G. Dūda would like to acknowledge support from the NASA Nebraska Space Consortium through Grant NNG05GJ03H.

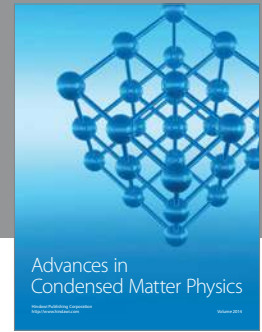
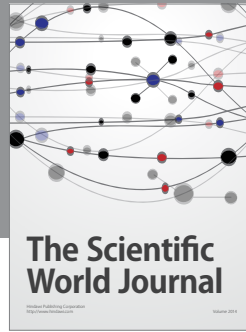
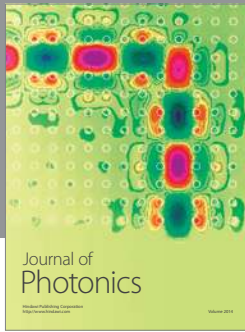
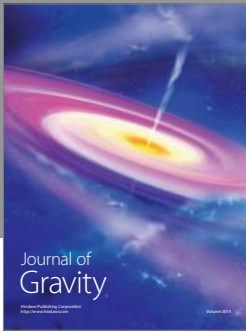
References

- [1] J. H. Oort, "The force exerted by the stellar system in the direction perpendicular to the galactic plane and some related problems," *Bulletin of the Astronomical Institutes of the Netherlands*, vol. 4, p. 249, 1932.
- [2] F. Zwicky, "Spectral displacement of extra galactic nebulae," *Helvetica Physica Acta*, vol. 6, pp. 110–127, 1933.
- [3] F. Zwicky, "On the masses of nebulae and clusters of nebulae," *The Astrophysical Journal*, vol. 86, pp. 217–246, 1937.
- [4] V. C. Rubin, "Dark matter in spiral galaxies," *Scientific American*, vol. 248, no. 6, pp. 96–108, 1983.
- [5] K. G. Begeman, "H I rotation curves of spiral galaxies," *Astronomy and Astrophysics*, vol. 223, pp. 47–60, 1989.
- [6] D. Walsh, R. F. Carswell, and R. J. Weymann, "0957+561 A, B: twin quasistellar objects or gravitational lens?" *Nature*, vol. 279, no. 5712, pp. 381–384, 1979.
- [7] R. Lynds and V. Petrosian, "Luminous arcs in clusters of galaxies," *The Astrophysical Journal*, vol. 336, pp. 1–8, 1989.
- [8] A. G. Bergmann, V. Petrosian, and R. Lynds, "Gravitational lens models of arcs in clusters," *Astrophysical Journal*, vol. 350, no. 1, pp. 23–35, 1990.
- [9] MOACollaboration, <http://www.phys.canterbury.ac.nz/mao/>.
- [10] OGLE Collaboration, <http://ogle.astrouw.edu.pl/>.
- [11] A. Becker et al., "The SuperMACHO microlensing survey," in *Gravitational Lensing Impact on Cosmology*, IAU Symposium no. 225, pp. 357–362, 2005.
- [12] C. Alcock, R. A. Allsman, D. R. Alves et al., "The MACHO project: microlensing results from 5.7 years of large magellanic cloud observations," *Astrophysical Journal*, vol. 542, no. 1, pp. 281–307, 2000.

- [13] P. Tisserand, L. Le Guillou, C. Afonso et al., "Limits on the MACHO content of the galactic halo from the EROS-2 survey of the magellanic clouds," *Astronomy and Astrophysics*, vol. 469, no. 2, pp. 387–404, 2007.
- [14] L. Kawano, NASA STI/Recon Technical Report 92, 25163, 1992.
- [15] R. H. Cyburt, "Primordial nucleosynthesis for the new cosmology: determining uncertainties and examining concordance," *Physical Review D*, vol. 70, no. 2, Article ID 023505, 2004.
- [16] A. A. Penzias and R. W. Wilson, "A measurement of excess antenna temperature at 4080 Mc/s," *The Astrophysical Journal*, vol. 142, pp. 419–421, 1965.
- [17] G. F. Smoot, C. L. Bennett, A. Kogut et al., "Structure in the COBE differential microwave radiometer first-year maps," *Astrophysical Journal*, vol. 396, no. 1, pp. L1–L5, 1992.
- [18] N. Jarosik et al., "Seven-year Wilkinson Microwave Anisotropy Probe (WMAP1) observations: sky maps, systematic errors, and basic results," <http://arxiv.org/abs/1001.4744>.
- [19] K. N. Abazajian, J. K. Adelman-McCarthy, M. A. Agüeros et al., "The seventh data release of the sloan digital sky survey," *Astrophysical Journal, Supplement Series*, vol. 182, no. 2, pp. 543–558, 2009.
- [20] D. J. Eisenstein, I. Zehavi, D. W. Hogg et al., "Detection of the baryon acoustic peak in the large-scale correlation function of SDSS luminous red galaxies," *Astrophysical Journal*, vol. 633, no. 2, pp. 560–574, 2005.
- [21] S. Cole, W. J. Percival, J. A. Peacock et al., "The 2dF galaxy redshift survey: power-spectrum analysis of the final data set and cosmological implications," *Monthly Notices of the Royal Astronomical Society*, vol. 362, no. 2, pp. 505–534, 2005.
- [22] W. J. Percival, B. A. Reid, D. J. Eisenstein et al., "Baryon acoustic oscillations in the sloan digital sky survey data release 7 galaxy sample," *Monthly Notices of the Royal Astronomical Society*, vol. 401, no. 4, pp. 2148–2168, 2010.
- [23] M. Boylan-Kolchin, V. Springel, S. D. M. White, A. Jenkins, and G. Lemson, "Resolving cosmic structure formation with the Millennium-II Simulation," *Monthly Notices of the Royal Astronomical Society*, vol. 398, no. 3, pp. 1150–1164, 2009.
- [24] T. Di Matteo, J. Colberg, V. Springel, L. Hernquist, and D. Sijacki, "Direct cosmological simulations of the growth of black holes and galaxies," *Astrophysical Journal*, vol. 676, no. 1, pp. 33–53, 2008.
- [25] P. J. E. Peebles, "Large-scale background temperature and mass fluctuations due to scale-invariant primeval perturbations," *The Astrophysical Journal*, vol. 263, pp. L1–L5, 1982.
- [26] A. Jenkins, C. S. Frenk, F. R. Pearce et al., "Evolution of structure in cold dark matter universes," *Astrophysical Journal*, vol. 499, no. 1, pp. 20–40, 1998.
- [27] D. Clowe, M. Bradač, A. H. Gonzalez et al., "A direct empirical proof of the existence of dark matter," *Astrophysical Journal*, vol. 648, no. 2, pp. L109–L113, 2006.
- [28] M. Bradač, S. W. Allen, T. Treu et al., "Revealing the properties of dark matter in the merging cluster MACS J0025.4-1222," *Astrophysical Journal*, vol. 687, no. 2, pp. 959–967, 2008.
- [29] M. J. Jee, H. C. Ford, G. D. Illingworth et al., "Discovery of a ringlike dark matter structure in the core of the galaxy cluster Cl 0024+17," *Astrophysical Journal*, vol. 661, no. 2, pp. 728–749, 2006.
- [30] C. Amsler, M. Doser, M. Antonelli et al., "Review of particle physics," *Physics Letters B*, vol. 667, no. 1–5, pp. 1–6, 2008.
- [31] Tevatron New Phenomena, Higgs working group, "Combined CDF and DZero upper limits on standard model Higgs-Boson production with up to 4.2 fb⁻¹ of data," in *Proceedings of the Moriond ElectroWeak Conference*, 2009.
- [32] J. R. Bond, G. Efstathiou, and J. Silk, "Massive neutrinos and the large-scale structure of the universe," *Physical Review Letters*, vol. 45, no. 24, pp. 1980–1984, 1980.
- [33] M. Iye, K. Ota, N. Kashikawa et al., "A galaxy at a redshift $z = 6.96$," *Nature*, vol. 443, no. 7108, pp. 186–188, 2006.
- [34] T. Kinoshita and M. Nio, "Improved α^4 term of the electron anomalous magnetic moment," *Physical Review D*, vol. 73, no. 1, Article ID 013003, 2006.
- [35] J. Wess and J. Bagger, *Supersymmetry and Supergravity*, Princeton University Press, 1992.
- [36] U. Amaldi, W. De Boer, and H. Fürstenau, "Comparison of grand unified theories with electroweak and strong coupling constants measured at LEP," *Physics Letters B*, vol. 260, no. 3-4, pp. 447–455, 1991.
- [37] J. Ellis, S. Kelley, and D. V. Nanopoulos, "Probing the desert using gauge coupling unification," *Physics Letters B*, vol. 260, no. 1-2, pp. 131–137, 1991.
- [38] P. Langacker and M. Luo, "Implications of precision electroweak experiments for mt, θ , $\sin^2\theta$, and grand unification," *Physical Review D*, vol. 44, no. 3, pp. 817–822, 1991.
- [39] T. Falk, K. A. Olive, and M. Srednicki, "Heavy sneutrinos as dark matter," *Physics Letters B*, vol. 339, no. 3, pp. 248–251, 1994.
- [40] L. J. Hall, T. Moroi, and H. Murayama, "Sneutrino cold dark matter with lepton-number violation," *Physics Letters B*, vol. 424, no. 3-4, pp. 305–312, 1998.
- [41] E. J. Chun, H. B. Kim, and J. E. Kim, "Dark matter in axino-gravitino cosmology," *Physical Review Letters*, vol. 72, no. 13, pp. 1956–1959, 1994.
- [42] S. Borgani, A. Masiero, and M. Yamaguchi, "Light gravitinos as mixed dark matter," *Physics Letters B*, vol. 386, no. 1–4, pp. 189–197, 1996.
- [43] R. D. Peccei and H. R. Quinn, "CP conservation in the presence of pseudoparticles," *Physical Review Letters*, vol. 38, no. 25, pp. 1440–1443, 1977.
- [44] G. Raffelt and A. Weiss, "Red giant bound on the axion-electron coupling reexamined," *Physical Review D*, vol. 51, no. 4, pp. 1495–1498, 1995.
- [45] L. D. Duffy, P. Sikivie, D. B. Tanner et al., "High resolution search for dark-matter axions," *Physical Review D*, vol. 74, no. 1, Article ID 012006, 2006.
- [46] K. Yamamoto et al., "The Rydberg-Atom-Cavity axion search," in *Proceedings of the 3rd International Conference on Dark Matter in Astro and Particle Physics (Dark '00)*, Heidelberg, Germany, July 2000.
- [47] S. A. Bonometto, F. Gabbiani, and A. Masiero, "Mixed dark matter from axino distribution," *Physical Review D*, vol. 49, no. 8, pp. 3918–3922, 1994.
- [48] T. Kaluza, "Zum unittsproblem in der physik," *Sitzungsberichte der Preussischen Akademie der Wissenschaften*, pp. 966–972, 1922.
- [49] O. Klein, "Quantentheorie und fnfdimensionale Relativittstheorie," *Zeitschrift fr Physik a Hadrons and Nuclei*, vol. 37, pp. 895–906, 1926.
- [50] N. Arkani-Hamed, S. Dimopoulos, and G. Dvali, "The hierarchy problem and new dimensions at a millimeter," *Physics Letters B*, vol. 429, no. 3-4, pp. 263–272, 1998.

- [51] L. Randall and R. Sundrum, "Large mass hierarchy from a small extra dimension," *Physical Review Letters*, vol. 83, no. 17, pp. 3370–3373, 1999.
- [52] T. Appelquist, H. C. Cheng, and B. A. Dobrescu, "Bounds on universal extra dimensions," *Physical Review D*, vol. 64, no. 3, Article ID 035002, 2001.
- [53] G. Servant and T. M. P. Tait, "Is the lightest Kaluza-Klein particle a viable dark matter candidate?" *Nuclear Physics B*, vol. 650, no. 1-2, pp. 391–419, 2003.
- [54] D. Hooper and S. Profumo, "Dark matter and collider phenomenology of universal extra dimensions," *Physics Reports*, vol. 453, no. 2–4, pp. 29–115, 2007.
- [55] S. Coleman, "Q-balls," *Nuclear Physics B*, vol. 262, no. 2, pp. 263–283, 1985.
- [56] J. A. R. Cembranos, A. Dobado, and A. L. Maroto, "Brane-world dark matter," *Physical Review Letters*, vol. 90, no. 24, Article ID 241301, 4 pages, 2003.
- [57] M. Holthausen and R. Takahashi, "GIMPs from extra dimensions," *Physics Letters B*, vol. 691, no. 1, pp. 56–59, 2010.
- [58] M. Schelke, *Supersymmetric dark matter: aspects of sfermion coannihilations*, Ph.D. thesis, Stockholm University, 2004.
- [59] P. Gondolo and G. Gelmini, "Compatibility of DAMA dark matter detection with other searches," *Physical Review D*, vol. 71, no. 12, Article ID 123520, 2005.
- [60] E. Kolb and M. Turner, *The Early Universe*, Westview Press, 1994.
- [61] J. Edsjö and P. Gondolo, "Neutralino relic density including coannihilations," *Physical Review D*, vol. 56, no. 4, pp. 1879–1894, 1997.
- [62] L. Baudis and H. V. Klapdor-Kleingrothaus, "Direct detection of non-baryonic dark matter," in *Proceedings of the Beyond the Desert*, 1999.
- [63] J. Carr, G. Lamanna, and J. Lvalle, "Indirect detection of dark matter," *Reports on Progress in Physics*, vol. 69, no. 8, pp. 2475–2512, 2006.
- [64] J. Diemand, M. Kuhlen, P. Madau et al., "Clumps and streams in the local dark matter distribution," *Nature*, vol. 454, no. 7205, pp. 735–738, 2008.
- [65] J. Engel and P. Vogel, "Neutralino inelastic scattering with subsequent detection of nuclear γ rays," *Physical Review D*, vol. 61, no. 6, Article ID 063503, 4 pages, 2000.
- [66] Z. Ahmed, D. S. Akerib, S. Arrenberg et al., "Search for weakly interacting massive particles with the first five-tower data from the cryogenic dark matter search at the Soudan Underground Laboratory," *Physical Review Letters*, vol. 102, no. 1, Article ID 011301, 2009.
- [67] V. N. Lebedenko, H. M. Araújo, E. J. Barnes et al., "Results from the first science run of the ZEPLIN-III dark matter search experiment," *Physical Review D*, vol. 80, no. 5, Article ID 052010, 2009.
- [68] J. Angle, E. Aprile, F. Arneodo et al., "First results from the XENON10 dark matter experiment at the gran sasso national laboratory," *Physical Review Letters*, vol. 100, no. 2, Article ID 021303, 2008.
- [69] The Dark Matter Plotter, <http://dmtools.brown.edu/>.
- [70] R. Bernabei et al., "DAMA results," in *Proceedings of the 10th International Workshop on Neutrino Telescopes*, 2003.
- [71] P. Gondolo and G. Gelmini, "Cosmic abundances of stable particles: improved analysis," *Nuclear Physics B*, vol. 360, no. 1, pp. 145–179, 1991.
- [72] R. F. Lang, "The CRESST-II experiment," in *Proceedings of the 43rd Rencontres de Moriond*, La Thuile, Italy, March 2008.
- [73] V. Sanglard, A. Benoit, L. Bergé et al., "Final results of the EDELWEISS-I dark matter search with cryogenic heat-and-ionization Ge detectors," *Physical Review D*, vol. 71, no. 12, Article ID 122002, 2005.
- [74] H. V. Klapdor-Kleingrothaus and I. V. Krivosheina, "Status of GENIUS-TF-II and TF-III-The long-term stability of naked detectors in liquid nitrogen," *Nuclear Instruments and Methods in Physics Research A*, vol. 566, no. 2, pp. 472–476, 2006.
- [75] P. L. Brink et al., "Beyond the CDMS-II dark matter search: SuperCDMS," in *Proceedings of the Texas Symposium on Relativistic Astrophysics*, 2005.
- [76] D. S. Akerib, M. S. Armel-Funkhouser, M. J. Attisha et al., "Limits on spin-dependent WIMP-nucleon interactions from the Cryogenic Dark Matter search," *Physical Review D*, vol. 73, no. 1, Article ID 011102, 2006.
- [77] M. Barnabé-Heider, M. Di Marco, P. Doane et al., "Improved spin-dependent limits from the PICASSO dark matter search experiment," *Physics Letters B*, vol. 624, no. 3-4, pp. 186–194, 2005.
- [78] G. J. Alner, H. M. Araújo, G. J. Arnison et al., "Limits on WIMP cross-sections from the NAIAD experiment at the Boulby Underground Laboratory," *Physics Letters B*, vol. 616, no. 1-2, pp. 17–24, 2005.
- [79] D. D. Dixon, D. H. Hartmann, E. D. Kolaczyk et al., "Evidence for a galactic gamma-ray halo," *New Astronomy*, vol. 3, no. 7, pp. 539–561, 1998.
- [80] L. Bergström, J. Edsjö, M. Gustafsson, and P. Salati, "Is the dark matter interpretation of the EGRET gamma excess compatible with antiproton measurements?" *Journal of Cosmology and Astroparticle Physics*, no. 5, Article ID 006, 2006.
- [81] P. Gondolo et al., "DarkSUSY v. 5.05 Manual and Long Description of Routines," <http://www.physto.se/~edsjo/darksusy/>.
- [82] M. Ackermann, J. Ahrens, X. Bai et al., "Limits to the muon flux from neutralino annihilations in the Sun with the AMANDA detector," *Astroparticle Physics*, vol. 24, no. 6, pp. 459–466, 2006.
- [83] R. Abbasi, Y. Abdou, M. Ackermann et al., "Limits on a muon flux from neutralino annihilations in the sun with the IceCube 22-string detector," *Physical Review Letters*, vol. 102, no. 20, Article ID 201302, 2009.
- [84] S. Desai, Y. Ashie, S. Fukuda et al., "Search for dark matter WIMPs using upward through-going muons in Super-Kamiokande," *Physical Review D*, vol. 70, no. 8, Article ID 083523, 2004.
- [85] S. W. Barwick, J. J. Beatty, C. R. Bower et al., "The high-energy antimatter telescope (HEAT): an instrument for the study of cosmic-ray positrons," *Nuclear Instruments and Methods in Physics Research A*, vol. 400, no. 1, pp. 34–52, 1997.
- [86] J. J. Beatty, A. Bhattacharyya, C. Bower et al., "New measurement of the cosmic-ray positron fraction from 5 to 15 GeV," *Physical Review Letters*, vol. 93, no. 24, Article ID 241102, 2004.
- [87] S. Haino, K. Abe, K. Anraku et al., "Progress of the BESS Superconducting Spectrometer," *Nuclear Instruments and Methods in Physics Research A*, vol. 518, no. 1-2, pp. 167–171, 2004.
- [88] O. Adriani, G. C. Barbarino, G. A. Bazilevskaya et al., "An anomalous positron abundance in cosmic rays with energies 1.5–100 GeV," *Nature*, vol. 458, no. 7238, pp. 607–609, 2009.
- [89] A. A. Abdo, M. Ackermann, M. Ajello et al., "Measurement of the cosmic ray e^+e^- spectrum from 20 GeV to 1 TeV with

- the fermi large area telescope,” *Physical Review Letters*, vol. 102, no. 18, Article ID 181101, 2009.
- [90] F. Aharonian, A. G. Akhperjanian, G. Anton et al., “Probing the ATIC peak in the cosmic-ray electron spectrum with H.E.S.S.,” *Astronomy and Astrophysics*, vol. 508, no. 2, pp. 561–564, 2009.
- [91] A. Klypin, A. V. Kravtsov, O. Valenzuela, and F. Prada, “Where are the missing galactic satellites?” *Astrophysical Journal*, vol. 522, no. 1, pp. 82–92, 1999.
- [92] B. Moore, T. Quinn, F. Governato, J. Stadel, and G. Lake, “Cold collapse and the core catastrophe,” *Monthly Notices of the Royal Astronomical Society*, vol. 310, no. 4, pp. 1147–1152, 1999.
- [93] R. Barkana and A. Loeb, “The photoevaporation of dwarf galaxies during reionization,” *Astrophysical Journal*, vol. 523, no. 1, pp. 54–65, 1999.
- [94] A. Fujita, M.-M. M. Low, A. Ferrara, and A. Meiksin, “Cosmological feedback from high-redshift dwarf galaxies,” *Astrophysical Journal*, vol. 613, no. 1, pp. 159–179, 2004.
- [95] M. Milgrom, “A modification of the Newtonian dynamics as a possible alternative to the hidden mass hypothesis,” *The Astrophysical Journal*, vol. 270, pp. 365–370, 1983.
- [96] R. H. Sanders and M. A. W. Verheijen, “Rotation curves of Ursa major galaxies in the context of modified newtonian dynamics,” *Astrophysical Journal*, vol. 503, no. 1, pp. 97–108, 1998.
- [97] R. H. Sanders and E. Noordermeer, “Confrontation of MODified Newtonian Dynamics with the rotation curves of early-type disc galaxies,” *Monthly Notices of the Royal Astronomical Society*, vol. 379, no. 2, pp. 702–710, 2007.
- [98] J. R. Brownstein and J. W. Moffat, “Galaxy rotation curves without nonbaryonic dark matter,” *Astrophysical Journal*, vol. 636, no. 2, pp. 721–741, 2006.
- [99] J. D. Bekenstein, “Relativistic gravitation theory for the modified Newtonian dynamics paradigm,” *Physical Review D*, vol. 70, no. 8, Article ID 083509, 28 pages, 2004.
- [100] R. H. Sanders, “Modified gravity without dark matter,” in *The Invisible Universe: Dark Matter and Dark Energy*, Lecture Notes in Physics, pp. 375–402, Springer, New York, NY, USA, 2005.
- [101] A. Aguirre, J. Schaye, and E. Quataert, “Problems for modified Newtonian dynamics in clusters and the Ly α forest?” *Astrophysical Journal*, vol. 561, no. 2, pp. 550–558, 2001.
- [102] A. Abramovici and Z. Vager, “Test of Newtons second law at small accelerations,” *Physical Review D*, vol. 34, no. 10, pp. 3240–3241, 1986.
- [103] J. H. Gundlach, S. Schlamminger, C. D. Spitzer et al., “Laboratory test of Newton’s second law for small accelerations,” *Physical Review Letters*, vol. 98, no. 15, Article ID 150801, 2007.
- [104] G. W. Angus, B. Famaey, and A. Diaferio, “Equilibrium configurations of 11 eV sterile neutrinos in MONDian galaxy clusters,” *Monthly Notices of the Royal Astronomical Society*, vol. 402, no. 1, pp. 395–408, 2010.



Hindawi

Submit your manuscripts at
<http://www.hindawi.com>

